# CHAPTER 6. KINETIC INVESTIGATION - RESULTS AND DISCUSSION

## 6.1 INTRODUCTION

In the preceding sections of this thesis the most favourable operating region for the silica alumina butene skeletal isomerisation catalyst were identified and the performance of the catalyst quantified near this optimum. Here, in Chapter 6, the results obtained while attempting to identify the intrinsic reaction mechanism are presented. During this investigation, not only mechanism with a single elementary reaction step, i.e., Langmuir Hinshelwood Hougen Watson type rate equations, but also those with multiple elementary reaction steps controlling the overall reaction rate were considered. Furthermore, as was done previously, by among others, Choudhary and Doraiswamy (1975:234) and Bianchi et al. (1994:556), the law of mass action was also included.

The bench scale reactor system was used to study the kinetics of the n-butene skeletal isomerisation reaction. Details of the reactor system, the operating and data manipulation procedures as well as the analytical techniques used were discussed in Chapter 3 and Appendices 1 and 2. Given here, in Chapter 6 are the results of the modelling studies performed while investigating the kinetics of the n-butene skeletal isomerisation reaction. For a discussion on the modelling procedure and data used during this investigation, see Chapter 5 and Appendix 5. The results obtained during the experimental investigations were discussed previously in Chapter 4 while a comprehensive review of the relevant literature is presented in Chapter 2.

## 6.2 N-BUTENE SKELETAL ISOMERISATION MODELLING

Bond isomerisation of the 1-butene to *cis*-2- and *trans*-2-butene may be achieved at room temperature over acidic catalysts (Condon, 1958:99) or thermally at temperatures between 345°C and 420°C, without the formation of by-products, i.e., at temperatures well below those used for skeletal isomerisation. The results recorded during this study, as discussed in Section 4.6, and those reported by Bianchi et al. (1994:554) and Simon et al. (1994:480)

confirm that before skeletal isomerisation occurs the partial pressure ratios of the linear butene isomers in the product gas, are as predicted from thermodynamics. Hence, as the linear butenes are at equilibrium, they may be treated as a single pseudo-homogeneous species, i.e., n-butene. This together with the favoured, mono-molecular, 1-butene bond and skeletal isomerisation mechanism as originally proposed by Choudhary (1979:39), and discussed in detail in Section 2.4.3.3, implies that the relevant steps involved in the transformation of n-butene to isobutene are as shown in Figure 6.1.

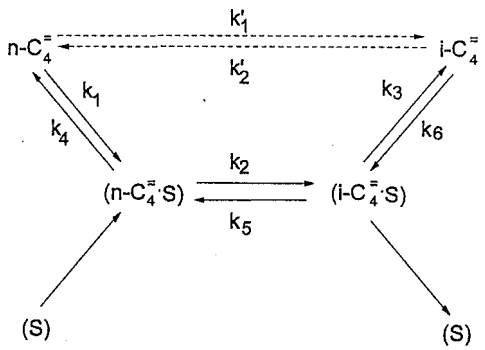


Figure 6.1 : n-Butene skeletal isomerisation reaction steps for the mono-molecular mechanism Case 2 to 8 (Solid lines) and the Mass Action Law - Case 1 (Dotted lines)

where

| | |
|---|---|
| (S) | represents a vacant surface site, -, |
| n-C4 | represents a molecule of n-butene in the gas phase, -, |
| i-C4 | represents a molecule of i-butene in the gas phase, -, |
| $(n\text{-}C_4^{=}\cdot S)$ | represents a molecule of n-butene on the surface of the catalyst, -, |
| $(i\text{-}C_4^{=}\cdot S)$ | represents a molecule of i-butene on the surface of the catalyst, -, |
| $k_i$ | are the frequency factors for Case 2 to Case 8, i=1 to 6, $mol\cdot kg^{-1}\cdot s^{-1}\cdot kPa^{-1}$ and |
| $k'_j$ | are the frequency factors for Case 1, j=1 or 2, $mol\cdot kg^{-1}\cdot s^{-1}\cdot kPa^{-1}$. |

By assuming the net reaction rates of one, two or all three of the reaction steps to be limiting the overall reaction rate, eight separate cases may be identified. The various cases considered during this study, including the mass action law are, with the bracketed values representing the number of rate limiting steps:

**Case 1** : Bulk reaction of n-butene to isobutene (1)

**Case 2** : Adsorption of n-butene (1)

**Case 3** : Surface reaction of n-butene to isobutene (1)

**Case 4** : Desorption of isobutene (1)

**Case 5** : Surface reaction of n-butene to isobutene plus desorption of isobutene (2)

**Case 6** : Adsorption of n-butene and desorption of isobutene (2)

**Case 7** : Adsorption of n-butene plus surface reaction of n-butene to isobutene (2)

**Case 8** : Adsorption of n-butene plus surface reaction of n-butene to isobutene plus desorption of isobutene (3)

The temperature dependency of the individual $k_i$, for i = 1 to 6 and $k_j$, for j = 1 to 2, values were in turn estimated using the Arrhenius equation, i.e.,

$$k_i = k_i^{o} \cdot \exp\left(\frac{-E_i}{R \cdot T}\right)$$

where

$k_i$ is the forward frequency factor for the reaction under consideration, $mol \cdot kg^{-1} \cdot s^{-1} \cdot kPa^{-1}$,

$k_i^{o}$ is the frequency factor for the reaction step under consideration, $mol \cdot kg^{-1} \cdot s^{-1} \cdot kPa^{-1}$,

$E_i$ is the activation energy for the reaction step under consideration, $cal \cdot mole^{-1}$,

R is the universal gas constant, R = 1.987 $cal \cdot mol^{-1} \cdot K^{-1}$,

T is the temperature, K and

i is the reaction under consideration, -.

By suitable manipulation of the individual reaction rate equations, together with a balance over the active sites, the corresponding multi-step kinetic equations could be derived. The nomenclature shown in Figure 6.1 and the equilibrium relationships $K_a = k_1 / k_2$, $K_s = k_2 / k_5$, $K_d = k_3 / k_6$ and $K = \{k_1 \cdot k_2 \cdot k_3\} / \{k_4 \cdot k_5 \cdot k_6\}$, were used in each case. Details of the derivation are shown in Appendix 3.

Using the full bench reactor data set, a total of 392 data points, as shown in Appendix 5, the optimum values of the unknown kinetic parameters, i.e., the rate constants for each of the reactions steps involved in the n-butene skeletal isomerisation reaction, were determined. To confirm that the values obtained in each case were the optimum values, the effect of perturbing each of the parameters in turn on the total error was investigated, i.e., confidence contours were generated. To allow discrimination between the rival models, the suitability of each of the cases considered in predicting the performance of the bench reactor system was quantified using a number of statistical procedures and by means of parity plots. The results obtained for each of the cases are presented individually with an overall discussion of the results obtained presented in Section .6.2.9

### 6.2.1 CASE 1 : MASS ACTION LAW

The mass action law is frequently used in the literature to describe the rate of n-butene skeletal isomerisation to isobutene (Choudhary and Doraiswamy, 1971:55, Bianchi et al., 1994:554, Simon et al., 1994:480, Szabo et al., 1993:319). The mass action law may be expressed, using the same nomenclature as before, by

$$r = k_1' \cdot P_{n\text{-}c_4^=} - k_2' P_{i\text{-}c_4^=} \qquad 6\text{-}2$$

To confirm that in each case the optimum values of the unknown parameters had been located, confidence contours were generated. As discussed in Chapter 5, Section 5.9.6, confidence contours were generated by determining the error while perturbing each of the parameters in turn. The confidence contour plots are shown in Figures 6.2 and 6.3 from which it may be seen that in all cases an optimum value was found. From an overall inspection, in the case of $E'_2$, it was found that increasing the value of the reverse reaction activation energy initially resulted in a rapid increase in the error, before this started to level off. With all else being held constant, increasing the absolute value of the activation energy results in a decrease in the reaction rate. Hence, as the reverse reaction rate becomes insignificant its mitigating effect on the overall error also becomes insignificant.

Hence, the trend observed is not totally unexpected.

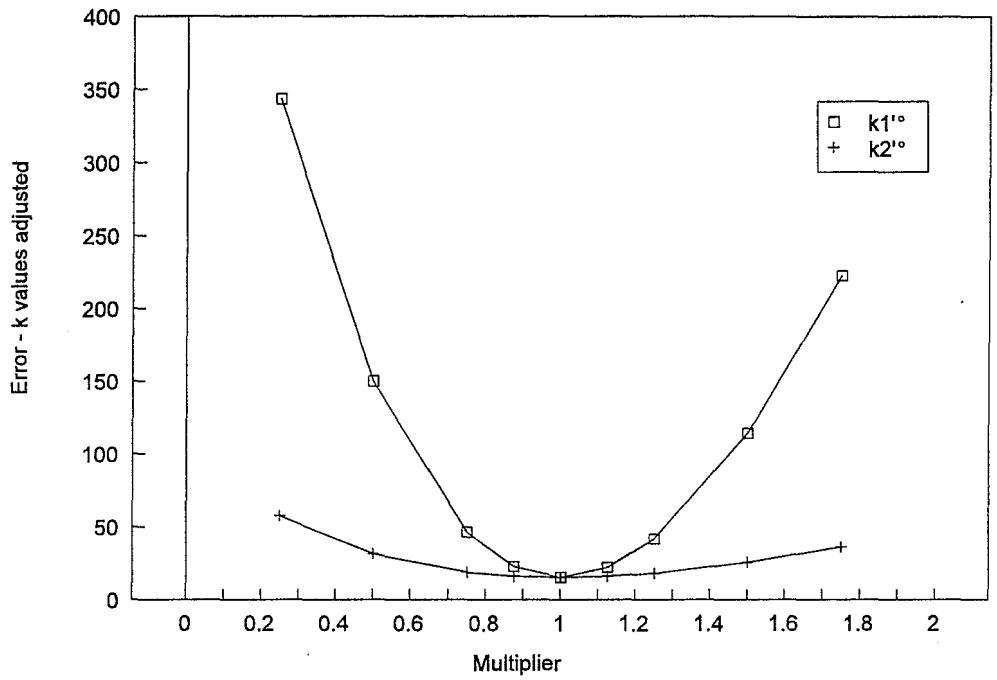


Figure 6.2 : Effect of adjusting individual $k_i°$ values on the overall percentage error when predicting the n-butene and isobutene partial pressures in the product gas for Case 1

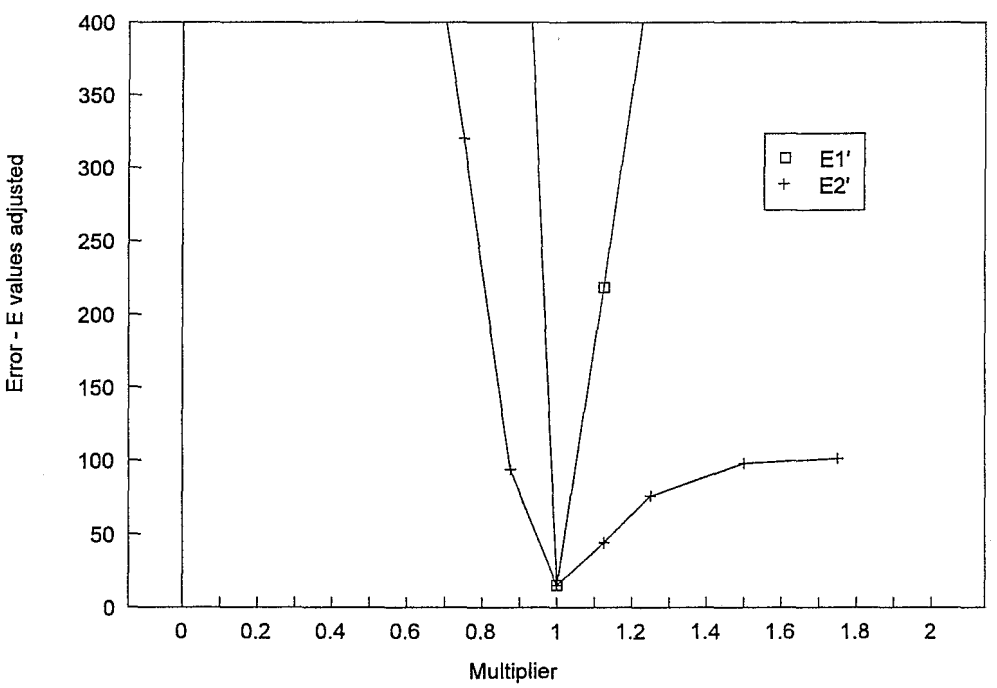


Figure 6.3 : Effect of adjusting individual E values on the overall percentage error in predicting the n-butene and isobutene partial pressures in the product gas - Case 1

Using the procedures discussed in Chapter 5, Section 5.8, the overall error, the lack of fit, the coefficient of determination and the confidence intervals were determined. These together with the optimum values of the unknown parameters, determined using the procedure discussed in Chapter 5 and Appendix 5 are shown in Table 6.1.

**TABLE 6.1 : OPTIMUM VALUES OF THE KINETIC PARAMETERS : CASE 1**

**Units :** Pre Exponential Factor, $k_j'^{o}$ = mol·kg$^{-1}$·s$^{-1}$·kPa$^{-1}$, Activation Energy $E_j'$ = cal·mol$^{-1}$

| Pre - exponential factors | | Activation Energy | |
|---|---|---|---|
| $k_1'^{o}$ | 0.095 (+7.93e-4 / -7.22e-4) | $E_1'$ | 11785 (+3.31 / -0.96) |
| $k_2'^{o}$ | 0.631 (+2.68e-2 / -2.48e-2) | $E_2'$ | 12979 (+25.7 / -94.5) |

| Statistical Parameter | $p_{n\text{-Butene}}$ | $p_{Isobutene}$ |
|---|---|---|
| Coefficient of Determination | 0.960 | 0.832 |
| Sum of Errors Squared | 0.761 | 9.658 |
| Lack of Fit | 0.339 < 1.0 Satisfactory fit | 0.83 < 1.0 Satisfactory fit |

The values of the forward ($E_1$ = 11785 cal·mole$^{-1}$ = 49.3 kJ·mole$^{-1}$) and reverse ($E_2$ = 12979 cal·mole$^{-1}$ = 54.33 kJ·mole$^{-1}$) activation energy are of a magnitude similar as those reported previously in the literature, as discussed in detail in Section 2.3.8. Nielsen et al. (1986:341) reported activation energies ranging from 67.8 kJ·mole$^{-1}$ to 113 kJ·mole$^{-1}$ over an alumina catalyst containing varying amounts of silica. Bianchi et al. (1994:554), using a boro-aluminosilicate zeolite, reported values ranging from 54.8 kJ·mole$^{-1}$ to 62.8 kJ·mole$^{-1}$ while Choudhary and Doraiswamy (1975:233) recorded a value of 35.2 kJ·mole$^{-1}$ over a fluorinated alumina catalyst. Furthermore, it was shown previously, in Chapter 5 and Appendix 4, using a combination of theoretical and experimental procedures, that intra- and inter-particle mass and heat transfer effects were not limiting the n-butene skeletal isomerisation reaction rate during this study. In view of these facts it may be concluded that the values of the activation energies shown in Table 6.1 represent the true intrinsic activation energy for the n-butene skeletal isomerisation reaction over the silica alumina catalyst used during this study.

To confirm the ability of Case 1 to predict the performance of the bench reactor system, parity plots of the actual and calculated n-butene and isobutene partial pressures in the

product gas were prepared, as shown in Figures 6.4 to 6.5. As may be seen from these, the mass action law is able to predict the performance of the bench reactor system.

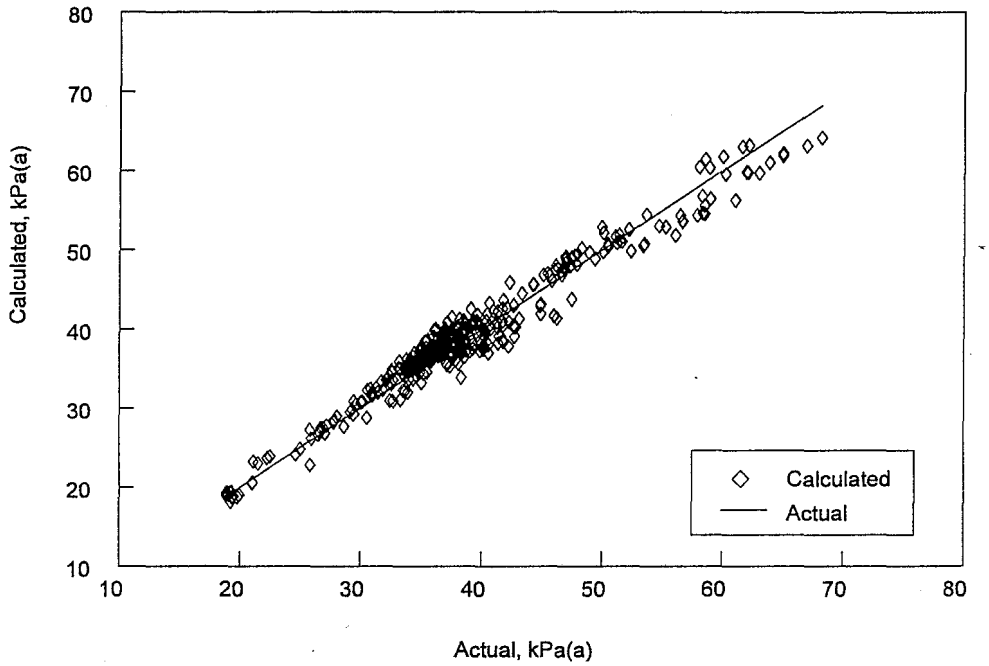


Figure 6.4 : Actual vs calculated n-butene partial pressure in the product gas - Case 1

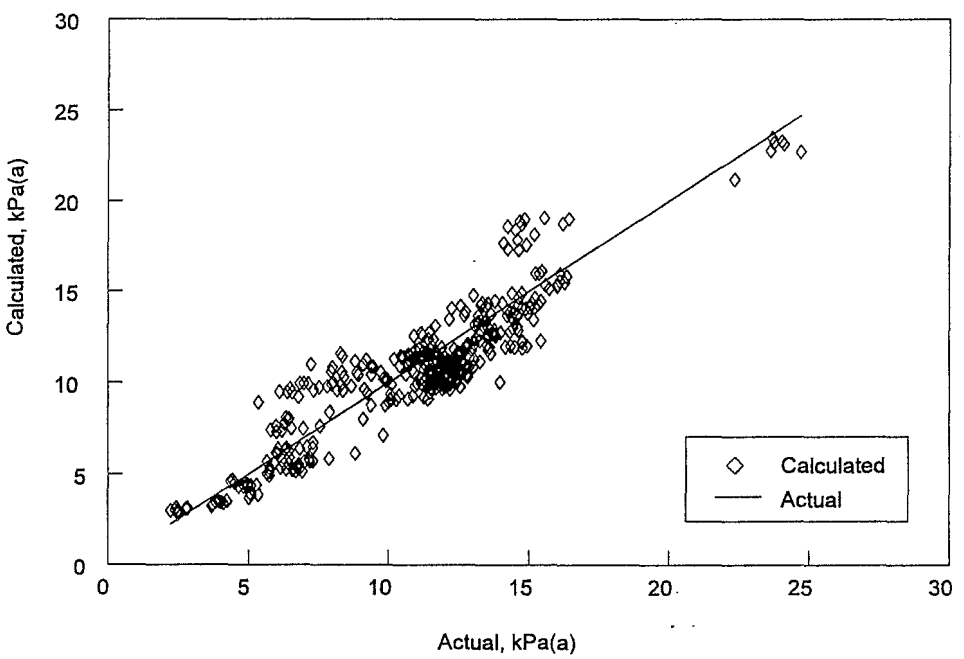


Figure 6.5 : Actual vs calculated isobutene partial pressure in the product gas - Case 1

### 6.2.2 CASE 2 : ADSORPTION OF N-BUTENE

For Case 2, it is assumed that the overall skeletal isomerisation rate is controlled by the net rate of the n-butene adsorption / desorption steps. The surface reactions and product desorption / adsorption steps are assumed to be at equilibrium. The overall rate equation for Case 2 was developed to give

$$r = \frac{(S)_t \cdot \left( P_{n\text{-}C_4^=} - \frac{P_{i\text{-}C_4^=}}{K} \right)}{\left( \frac{1}{k_1} \right) + \left( \frac{K_s + 1}{k_1 \cdot K_s} \right) \cdot \frac{P_{i\text{-}C_4^=}}{K_d}} \qquad 6\text{-}3$$

Using the same procedures, as before the optimum values of the unknown parameters were determined and the statistical parameters evaluated, as shown in Table 6.2. Also, the confidence contours and parity plots were generated and are shown in Figures 6.6 to 6.7 and Figures 6.8 to 6.9, respectively.

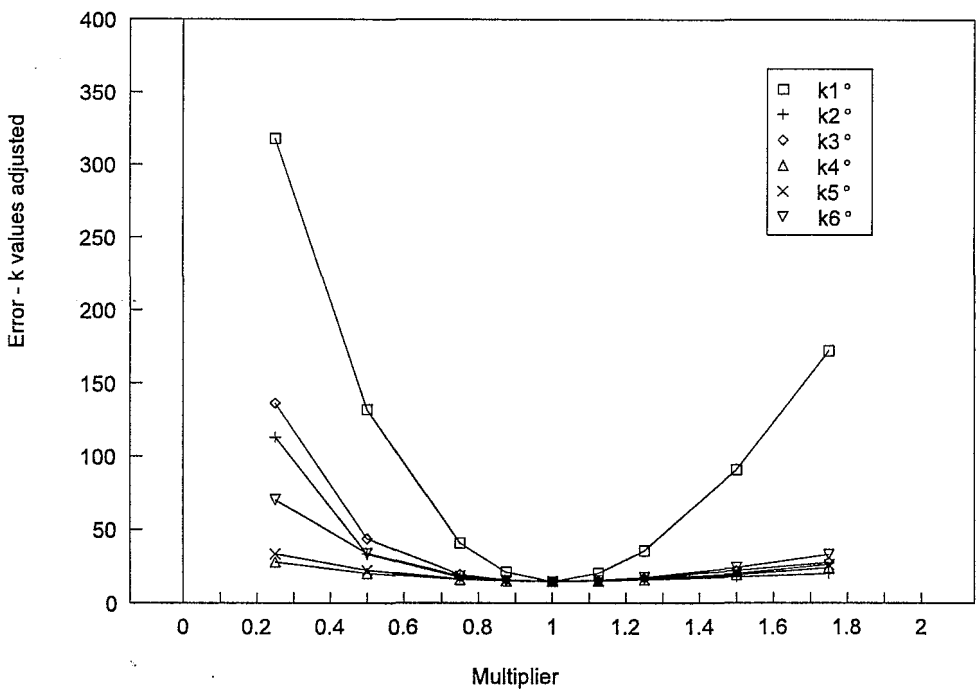


Figure 6.6 : Effect of adjusting individual $k_i°$ values on the overall percentage error when predicting the n-butene and isobutene partial pressures in the product gas for Case 2

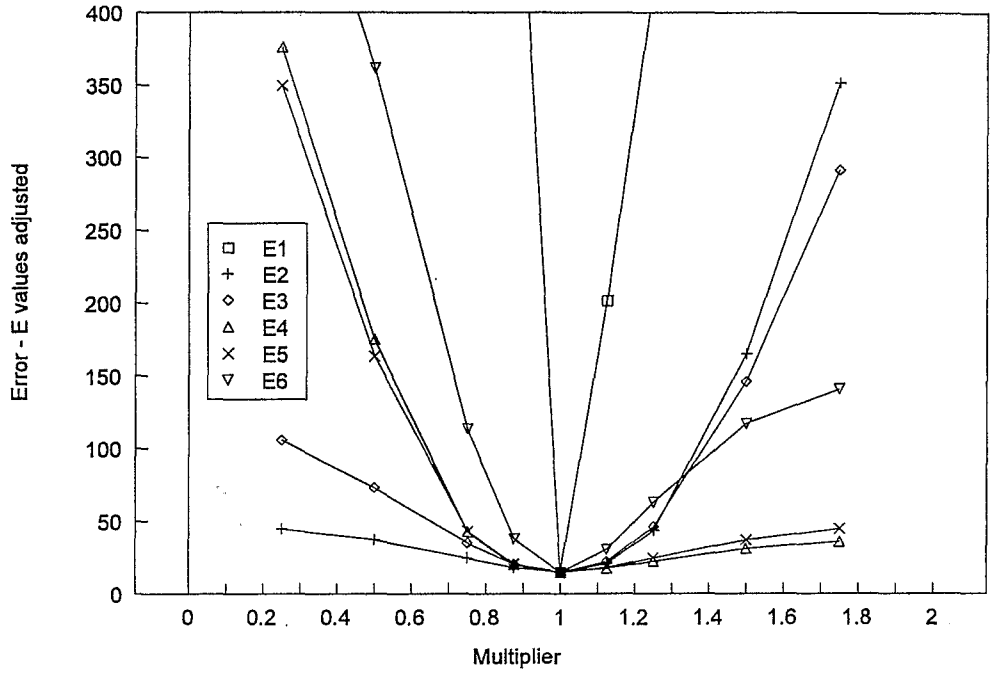


Figure 6.7 : Effect of adjusting individual E values on the overall percentage error in predicting the n-butene and isobutene partial pressures in the product gas - Case 2

From a closer inspection of Figure 6.6, and Figure 6.7 it may be seen that as the value of $k_1°$ and $E_1$ (n-butene adsorption step) were increased, the error recorded first decreases before increasing again. This symmetrical result indicates that specific values for $k_1°$ and $E_1$ are required to minimise the error. From this it may be concluded that the values of the unknown parameters determined are the optimum values and that this reaction step, the adsorption of n-butene, is a significant step. Examining the effects of adjusting the values of $k_i°$ with i=2 to 6, on the error showed that although optimum values were found in each case, these were less sensitive to an increase in the reaction rate than to a decrease in the reaction rate. This may suggest that the ability of the model in predicting the actual performance of the system is not as sensitive to the values of $k_2°$ to $k_6°$ as long as these are larger than some limiting value. The picture becomes much clearer when examining the shape of the confidence contours generated for the activation energies. In the case of the forward reactions, increasing the activation energies $E_2$ (n-butene to isobutene surface reaction step) and $E_3$ (isobutene desorption step) beyond the optimum value results in a dramatic increase in the error, while decreasing the values has a much smaller effect on the error. As, with all else being held constant, increasing the absolute value of

the activation energy will result in a exponential decrease in the reaction rate, it may be concluded that this suggests that the forward reaction rates must exceed some limiting value. Conversely, the shape of the confidence contours for the activation energies $E_4$ (n-butene desorption) and $E_5$ (isobutene to n-butene surface reaction step) for the corresponding reverse reactions, suggest that these must be slower than some limiting value. The optimum values of the various parameters together with the results from the various statistical tests performed are shown in Table 6.2.

**TABLE 6.2 : OPTIMUM VALUES OF THE KINETIC PARAMETERS : CASE 2**

**Units :** Pre Exponential Factor, $k_i^\circ$ = mol·kg$^{-1}$·s$^{-1}$·kPa$^{-1}$, Activation Energy $E_i$ = cal·mol$^{-1}$

| Pre - exponential factors | | Activation Energy | |
|---|---|---|---|
| $k_1^\circ$ | 0.119 (+1.22e-3 / -1.08e-3) | $E_1$ | 12015 (+3.57 / -1.22) |
| $k_2^\circ$ | 5.366 (+9.37e-1 / -6.10e-1) | $E_2$ | 5281 (+51.0 / -89.6) |
| $k_3^\circ$ | 1.060 (+8.8e-2 / -6.22e-2) | $E_3$ | 4569 (+34.6 / - 43.7) |
| $k_4^\circ$ | 0.328 (+6.15e-2 / -5.85e-2) | $E_4$ | 5537 (+11.6 / -58.7) |
| $k_5^\circ$ | 1.505 (+2.22e-1 / -2.07e-1) | $E_5$ | 5260 (+89.9 / - 51.3) |
| $k_6^\circ$ | 0.249 (+1.90e-2 / -1.61e-2) | $E_6$ | 7931 (+27.8 / - 18.9) |

| Parameter | $p_{n\text{-Butene}}$ | $p_{Isobutene}$ |
|---|---|---|
| Coefficient of Determination | 0.961 | 0.842 |
| Sum of Errors Squared | 0.776 | 9.215 |
| Lack of Fit | 0.343 < 1.0 Satisfactory fit | 0.796 < 1.0 Satisfactory fit |

To confirm the ability of Case 2 to predict the performance of the bench reactor system, parity plots of the actual and calculated n-butene and isobutene partial pressures in the product gas were prepared, as shown in Figures 6.8 to 6.9, from which it may be seen that Case 2 is also capable in predicting the performance of the bench reactor system with respect to the n-butene and isobutene partial pressures in the product gas.

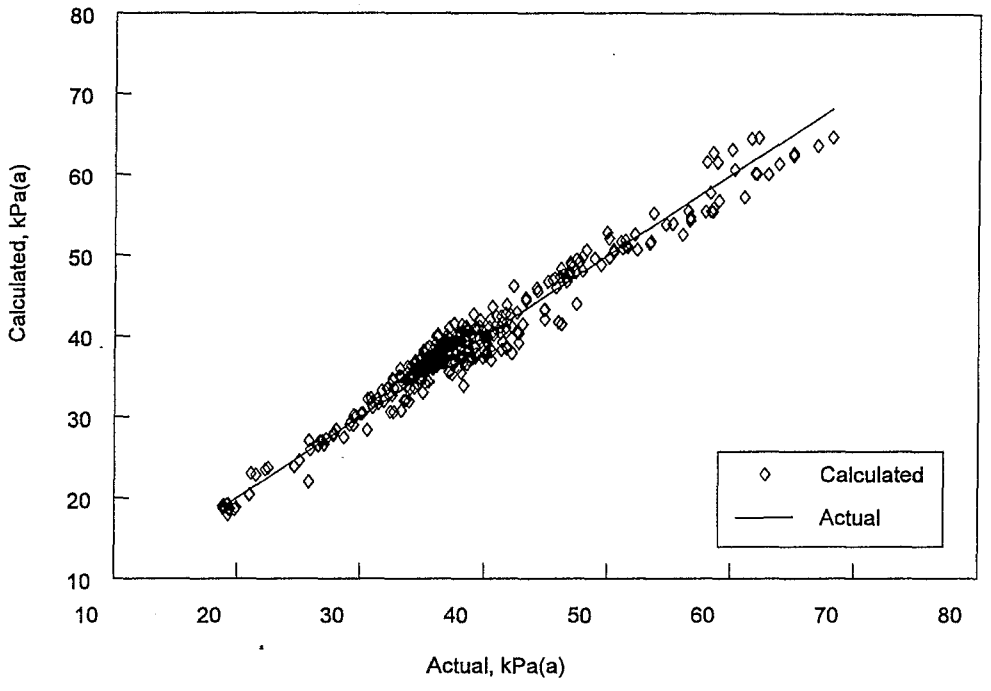


Figure 6.8 : Actual vs calculated n-butene partial pressure in the product gas - Case 2

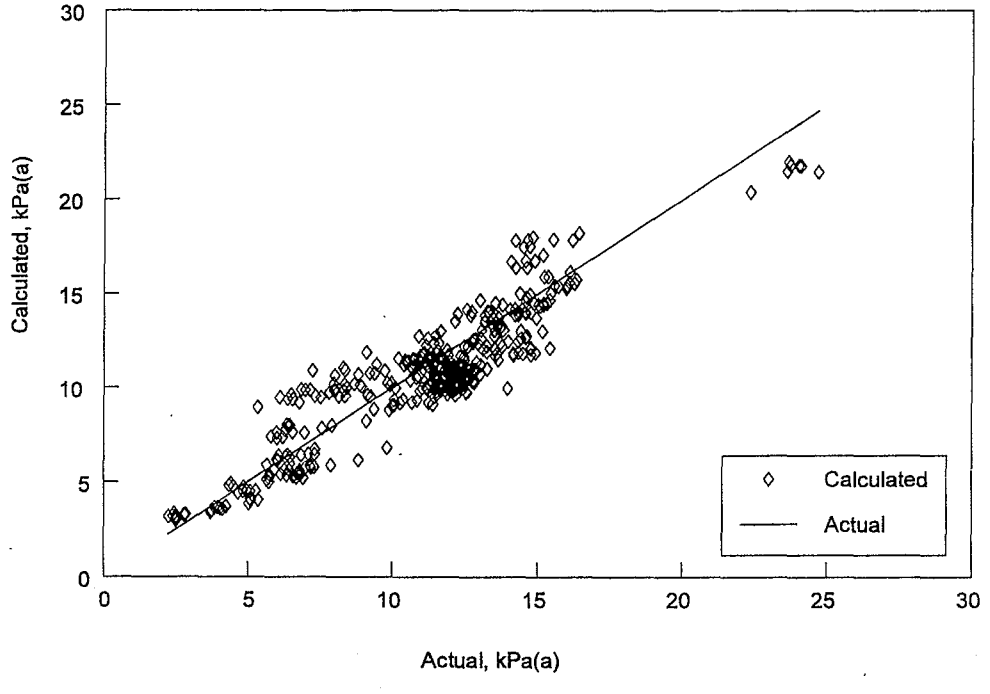


Figure 6.9 : Actual vs calculated isobutene partial pressure in the product gas - Case 2

### 6.2.3 CASE 3 : SURFACE REACTION OF N-BUTENE TO ISOBUTENE

For Case 3, it is assumed that the overall skeletal isomerisation rate is controlled by the net surface reaction rate of n-butene to isobutene. The n-butene adsorption / desorption and isobutene desorption / adsorption reactions are assumed to be at equilibrium. The overall rate equation for Case 3 was developed to give

$$r = \frac{(S)_t \cdot \left( P_{n\text{-}c_4^=} - \frac{P_{i\text{-}c_4^=}}{K} \right)}{\left( \frac{1}{k_2 \cdot K_a} \right) + \left( \frac{1}{k_2 \cdot K_a} \right) \cdot K_a \cdot P_{n\text{-}c_4^=} + \left( \frac{1}{k_2 \cdot K_a} \right) \cdot \frac{P_{i\text{-}c_4^=}}{K_d}} \qquad 6\text{-}4$$

The optimum values of the unknown parameters and statistical parameters evaluated are shown in Table 6.3. The confidence contours and parity plots are shown in Figures 6.10 to 6.11 and Figures 6.12 to 6.13 respectively.

**TABLE 6.3 : OPTIMUM VALUES OF THE KINETIC PARAMETERS : CASE 3**

**Units :** Pre Exponential Factor, $k_j^\circ$ = mol·kg$^{-1}$·s$^{-1}$·kPa$^{-1}$, Activation Energy $E_j$ = cal·mol$^{-1}$

| Pre - exponential factors | | Activation Energy | |
|---|---|---|---|
| $k_1^\circ$ | 0.111 (+1.13e-3 / -1.01e-3) | $E_1$ | 10975 (+3.70 / -1.40) |
| $k_2^\circ$ | 2.683 (+2.58e-2 / -2.31e-2) | $E_2$ | 5826 (+5.20 / -3.01) |
| $k_3^\circ$ | 1.529 (+1.27e-1 / -9.19e-2) | $E_3$ | 3533 (+46.3 / -56.1) |
| $k_4^\circ$ | 1.446 (+1.66e-2 / -1.13e-2) | $E_4$ | 3939 (+5.14 / -7.30) |
| $k_5^\circ$ | 0.305 (+4.74e-2 / -4.25e-2) | $E_5$ | 7286 (+76.6 / -33.8) |
| $k_6^\circ$ | 0.731 (+5.71e-2 / -4.74e-2) | $E_6$ | 8017 (+28.6 / - 18.6) |

| Parameter | $p_{n\text{-Butene}}$ | $p_{Isobutene}$ |
|---|---|---|
| Coefficient of Determination | 0.961 | 0.842 |
| Sum of Errors Squared | 0.771 | 9.244 |
| Lack of Fit | 0.341 < 1.0 Satisfactory fit | 0.795 < 1.0 Satisfactory fit |

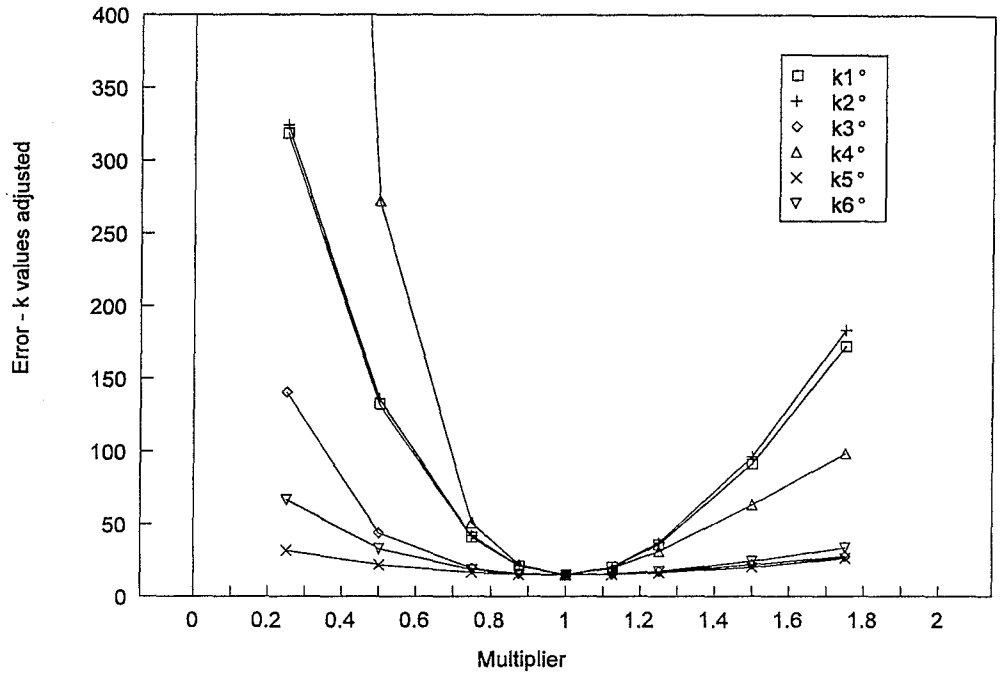


Figure 6.10 : Effect of adjusting individual $k_i°$ values on the overall percentage error when predicting the n-butene and isobutene partial pressures in the product gas for Case 3

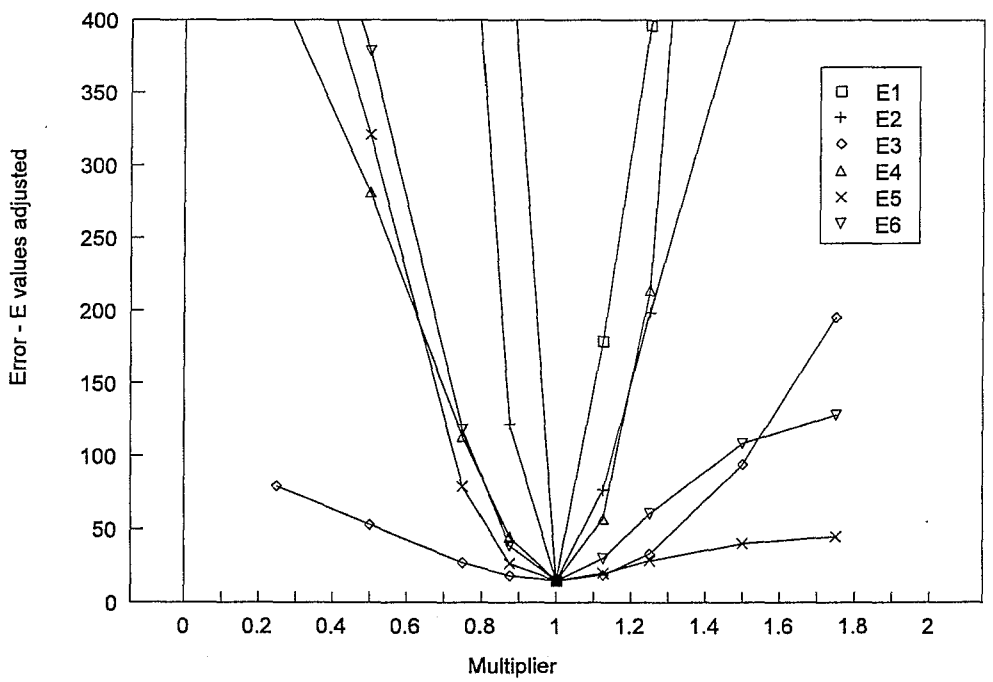


Figure 6.11 : Effect of adjusting individual E values on the overall percentage error in predicting the n-butene and isobutene partial pressures in the product gas - Case 3

In this case, a closer inspection of Figure 6.10 and 6.11 suggests, from the symmetry of the curves, that the true optimum values were once again located for $k_1°$ to $k_6°$ and necessarily for $E_1$ to $E_6$. However, the overall trends in the confidence contours recorded for $k_5°$ and $k_6°$, taken in combination with the trends observed for $E_5$ and $E_6$ suggest that the rate of these reverse reactions must be smaller than some limiting value while the overall shape of the confidence contour for $k_3°$ and $E_3$ suggests that the rate of this forward reaction must be faster than some limiting value, as was concluded previously.

To visually confirm the ability of Case 3 to predict the performance of the bench reactor system, parity plots of the actual and calculated n-butene and isobutene partial pressures in the product gas were prepared, as shown in Figures 6.12 and 6.13. As may be seen from these figures Case 3 is also capable of predicting the performance of the bench reactor system with respect to the n-butene and isobutene partial pressures in the product gas.

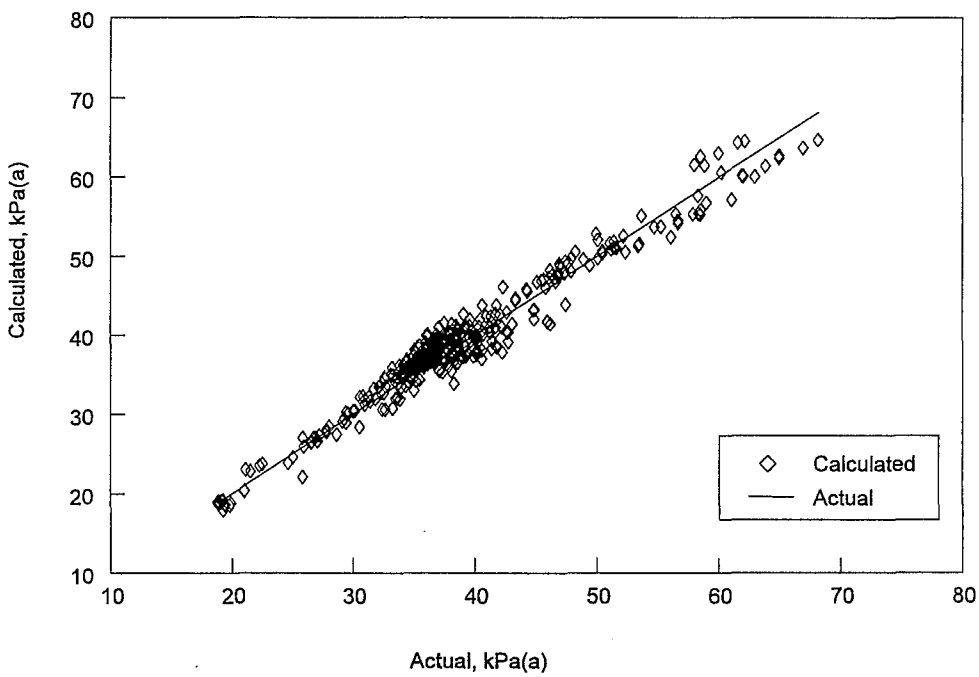


Figure 6.12 : Actual vs calculated n-butene partial pressure in the product gas - Case 3

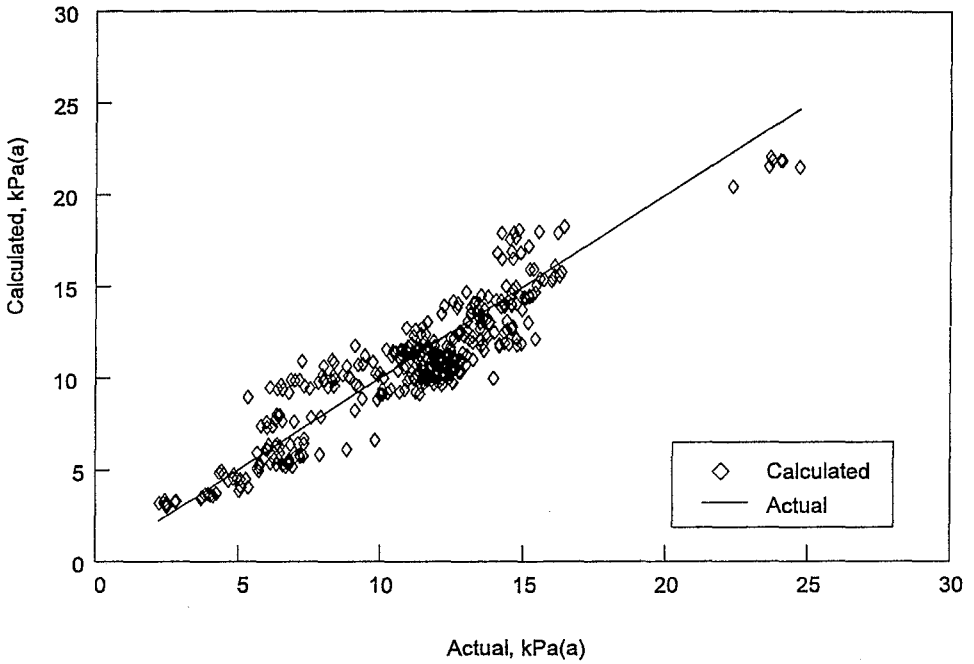


Figure 6.13 : Actual vs calculated isobutene partial pressure in the product gas - Case 3

### 6.2.4 CASE 4 : DESORPTION OF ISOBUTENE

For Case 4, it is assumed that the overall skeletal isomerisation rate is controlled by the net rate of the isobutene desorption / adsorption steps. The n-butene adsorption / desorption and n-butene / isobutene surface reaction steps are assumed to be at equilibrium. The overall rate equation for Case 4 was developed to give

$$r = \frac{(S)_t \cdot \left( P_{n\text{-}C_4^=} - \frac{P_{i\text{-}C_4^=}}{K} \right)}{\left( \frac{1}{k_6 \cdot K} \right) + \left( \frac{1 + K_s}{k_6 \cdot K} \right) \cdot K_a \cdot P_{n\text{-}C_4^=}} \qquad 6\text{-}7$$

The optimum values of the unknown parameters and statistical parameters evaluated are shown in Table 6.4. The confidence contours and parity plots are shown in Figures 6.14 to 6.15 and Figures 6.16 to 6.17 respectively.

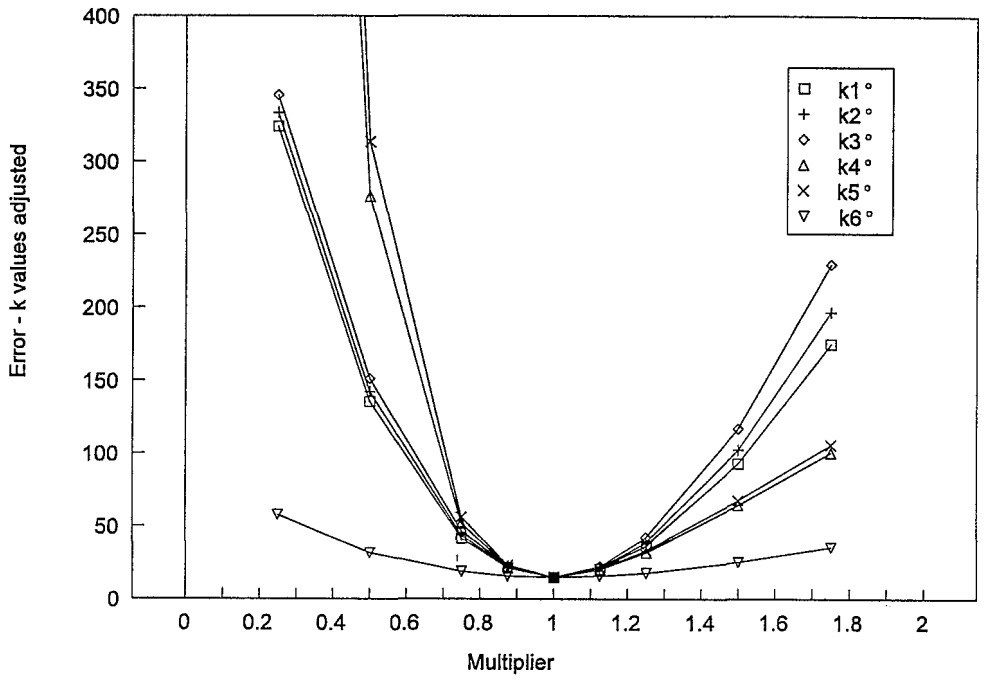


Figure 6.14 : Effect of adjusting individual $k_i°$ values on the overall percentage error when predicting the n-butene and isobutene partial pressures in the product gas for Case 4

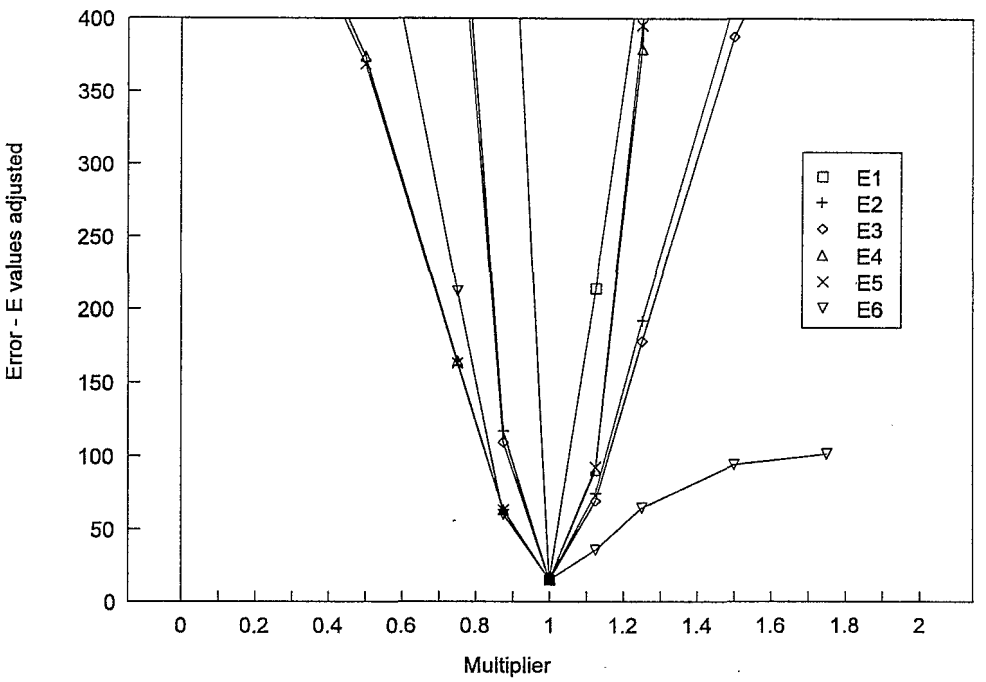


Figure 6.15 : Effect of adjusting individual E values on the overall percentage error in predicting the n-butene and isobutene partial pressures in the product gas - Case 4

Form an inspection of Figure 6.14 and Figure 6.15 it may be seen that for each parameter the optimum value for was located. Furthermore, the confidence contours for $k_1°$ to $k_5°$ and necessarily $E_1$ to $E_5$, are symmetrical about the optimum values determined. In the case of Step 6 (isobutene adsorption) an overall inspection of the confidence contour recorded for the activation energy of this reverse reaction step suggests that the rate must be smaller than some limiting value. The optimum values of the unknown parameters together with the confidence intervals and the statistical parameters evaluated to quantify the degree of fit are shown in Table 6.4.

To visually confirm the ability of Case 4 to predict the performance of the bench reactor system, parity plots of the actual and calculated n-butene and isobutene partial pressures in the product gas were prepared, as shown in Figures 6.16 and 6.17. It may be concluded that Case 4 is also capable in predicting the performance of the bench reactor system with respect to the n-butene and isobutene partial pressures in the product gas.

**TABLE 6.4 : OPTIMUM VALUES OF THE KINETIC PARAMETERS : CASE 4**

**Units :** Pre Exponential Factor, $k_j° = mol \cdot kg^{-1} \cdot s^{-1} \cdot kPa^{-1}$, Activation Energy $E_j = cal \cdot mol^{-1}$

| Pre - exponential factors | | Activation Energy | |
|---|---|---|---|
| $k_1°$ | 0.075 (+7.50e-4 / -6.72e-4) | $E_1$ | 12396 (+3.49 / -1.20) |
| $k_2°$ | 3.787 (+3.43e-2 / -3.11e-2) | $E_2$ | 5518 (+5.19 / -3.03) |
| $k_3°$ | 0.679 (+5.41e-3 / -5.00e-3) | $E_3$ | 4980 (+5.12 / -2.95) |
| $k_4°$ | 0.456 (+5.20e-3 / -3.51e-3) | $E_4$ | 5079 (+3.77 / -5.91) |
| $k_5°$ | 1.850 (+1.94e-2 / -1.29e-2) | $E_5$ | 4875 (+3.53 / -5.68) |
| $k_6°$ | 0.070 (+5.36e-3 / -4.57e-3) | $E_6$ | 10130 (+27.7 / - 12.6) |

| Parameter | $p_{n\text{-Butene}}$ | $p_{Isobutene}$ |
|---|---|---|
| Coefficient of Determination | 0.961 | 0.842 |
| Sum of Errors Squared | 0.769 | 9.406 |
| Lack of Fit | 0.339 < 1.0 Satisfactory fit | 0.798 < 1.0 Satisfactory fit |

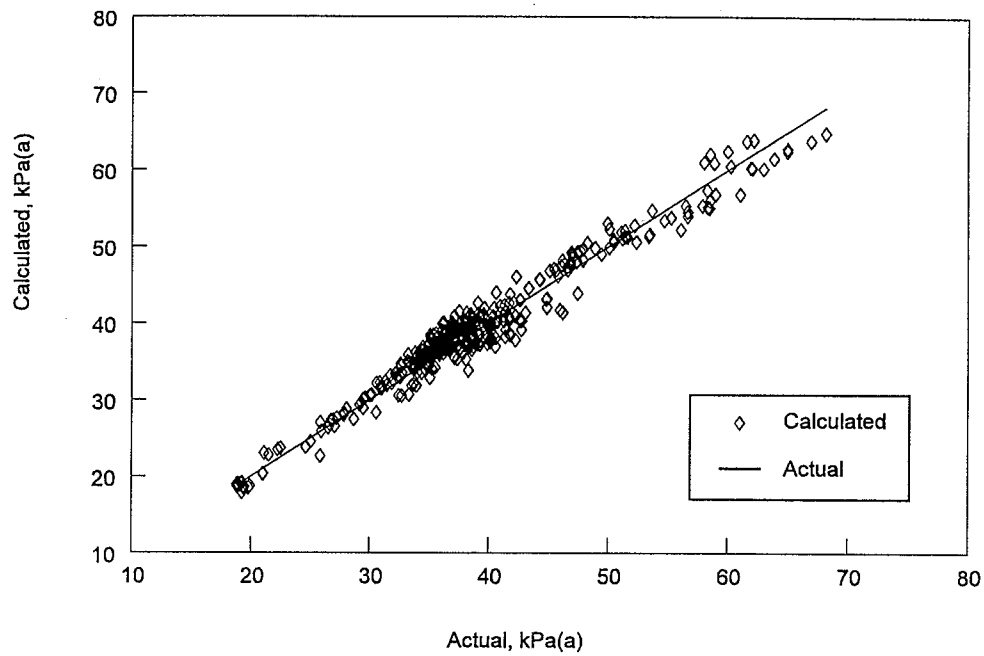


Figure 6.16 : Actual vs calculated n-butene partial pressure in the product gas - Case 4

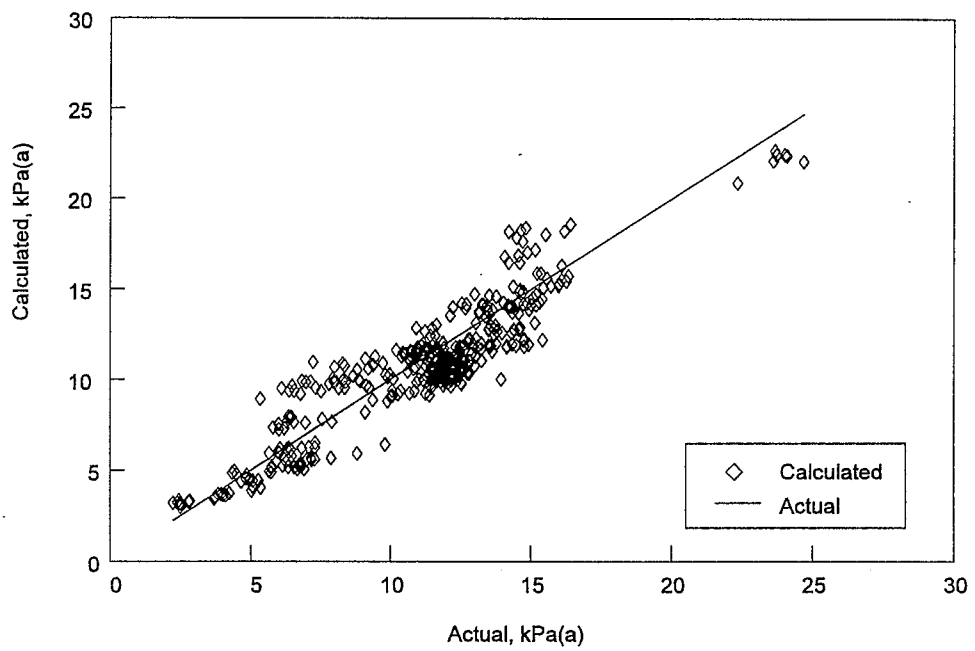


Figure 6.17 : Actual vs calculated isobutene partial pressure in the product gas - Case 4

### 6.2.5 CASE 5 : SURFACE REACTION OF N-BUTENE TO ISOBUTENE PLUS DESORPTION OF ISOBUTENE

For Case 5, it is assumed that the overall skeletal isomerisation rate is controlled by the net rate of the surface reaction of the n-butene to isobutene and by the desorption / adsorption of the isobutene. The n-butene adsorption / desorption reactions are assumed to be at equilibrium. The overall rate equation for Case 5 was developed to give

$$r = \frac{(S)_t \cdot \left( P_{n\text{-}c_4^=} - \frac{P_{i\text{-}c_4^=}}{K} \right)}{\left( \frac{1}{k_6 \cdot K} + \frac{1}{k_2 \cdot K_a} \right) + \left( \frac{1 + K_s}{k_6 \cdot K} + \frac{1}{k_2 \cdot K_a} \right) \cdot K_a \cdot P_{n\text{-}c_4^=} + \left( \frac{1}{k_2 \cdot K_a} \right) \cdot \frac{P_{i\text{-}c_4^=}}{K_d}} \qquad 6\text{-}8$$

The optimum values of the unknown parameters and statistical parameters evaluated are shown in Table 6.5. The confidence contours and parity plots are shown in Figures 6.18 and 6.19 and Figures 6.20 to 6.21 respectively.

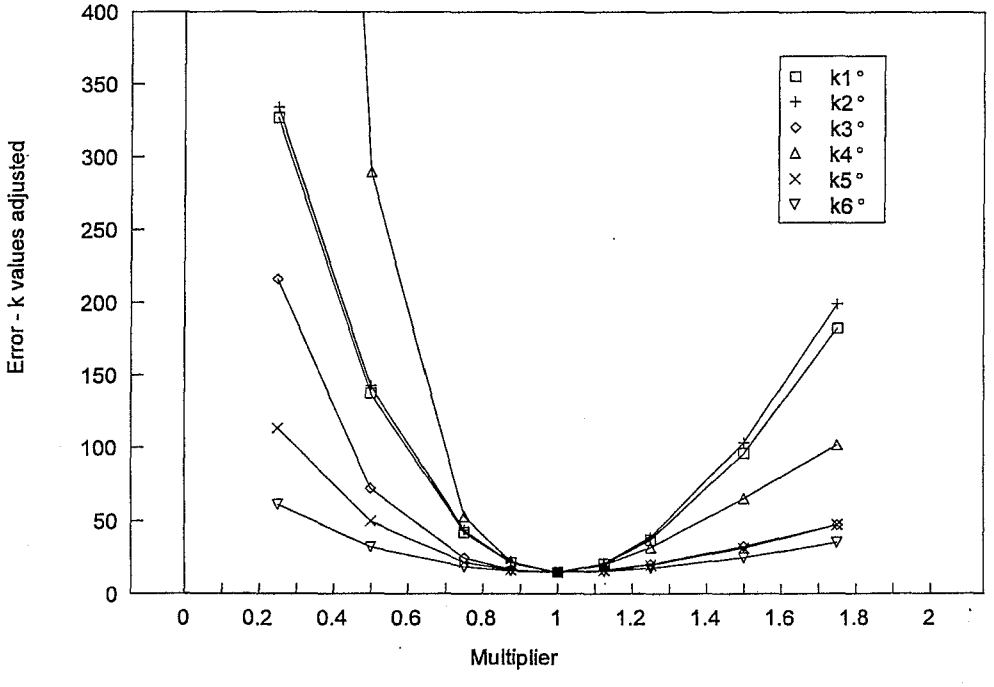


Figure 6.18 : Effect of adjusting individual $k_i°$ values on the overall percentage error when predicting the n-butene and isobutene partial pressures in the product gas for Case 5

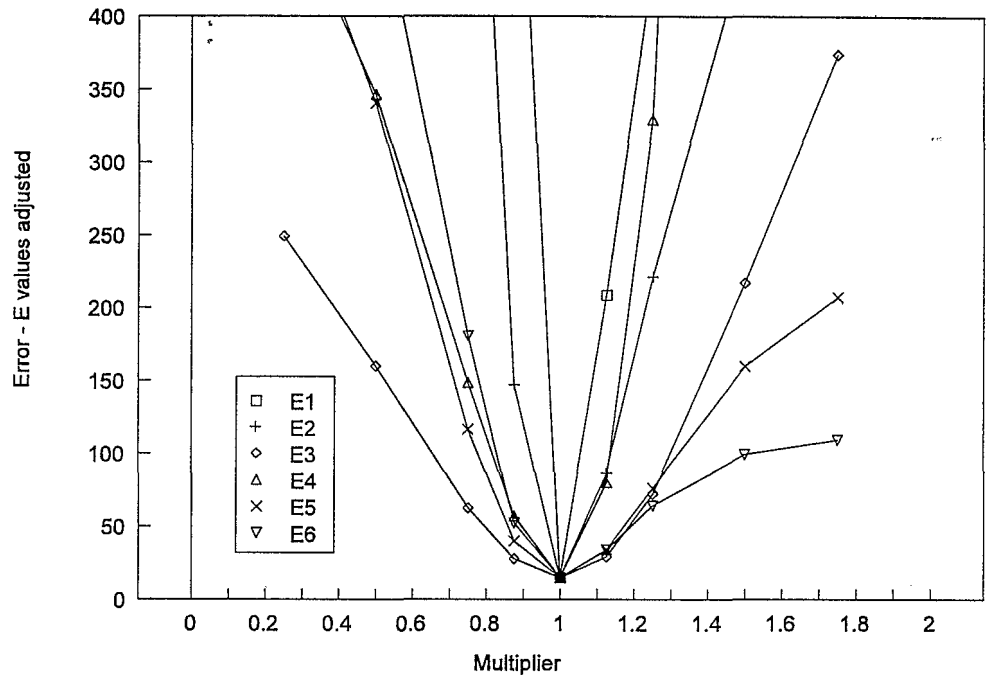


Figure 6.19 : Effect of adjusting individual E values on the overall percentage error in predicting the n-butene and isobutene partial pressures in the product gas - Case 5

From a global inspection of Figure 6.18, and Figure 6.19 it may be seen that the confidence contours, with the exception of that for $E_6$ are clearly symmetrical about the optimum values located. From an overall inspection of the confidence contour, for the activation energy of the isobutene adsorption reaction, $E_6$, it may be concluded that the rate of this reaction must be smaller than some limiting value.

The optimum values of the unknown parameters and the results from the statistical evaluations are shown in Table 6.5. The ability for Case 5 to predict the performance of the bench reactor system was further confirmed by means of the parity plots shown in Figures 6.20 and 6.21. Close agreement between the actual and calculated n-butene and isobutene partial pressures in the product gas were obtained.

**TABLE 6.5 : OPTIMUM VALUES OF THE KINETIC PARAMETERS : CASE 5**

**Units :** Pre Exponential Factor, $k_j^\circ$ = mol·kg$^{-1}$·s$^{-1}$·kPa$^{-1}$, Activation Energy $E_j$ = cal·mol$^{-1}$

| Pre - exponential factors | | Activation Energy | |
|---|---|---|---|
| $k_1^\circ$ | 0.066 (+6.39e-4 / -5.74e-4) | $E_1$ | 12034 (+3.46 / -1.17) |
| $k_2^\circ$ | 3.193 (+2.85e-2 / -2.59e-2) | $E_2$ | 6148 (+4.77 / -2.59) |
| $k_3^\circ$ | 0.926 (+3.26e-2 / -2.49e-2) | $E_3$ | 4416 (+17.0 / -18.8) |
| $k_4^\circ$ | 0.514 (+5.66e-3 / -3.81e-3) | $E_4$ | 4663 (+3.99 / -6.13) |
| $k_5^\circ$ | 0.915 (+3.88e-2 / -3.21e-2) | $E_5$ | 6303 (+18.2 / -13.9) |
| $k_6^\circ$ | 0.177 (+1.33e-2 / -1.13e-2) | $E_6$ | 9397 (+27.3 / - 13.9) |

| Parameter | $p_{n\text{-Butene}}$ | $p_{Isobutene}$ |
|---|---|---|
| Coefficient of Determination | 0.961 | 0.842 |
| Sum of Errors Squared | 0.769 | 9.347 |
| Lack of Fit | 0.340 < 1.0 Satisfactory fit | 0.800 < 1.0 Satisfactory fit |

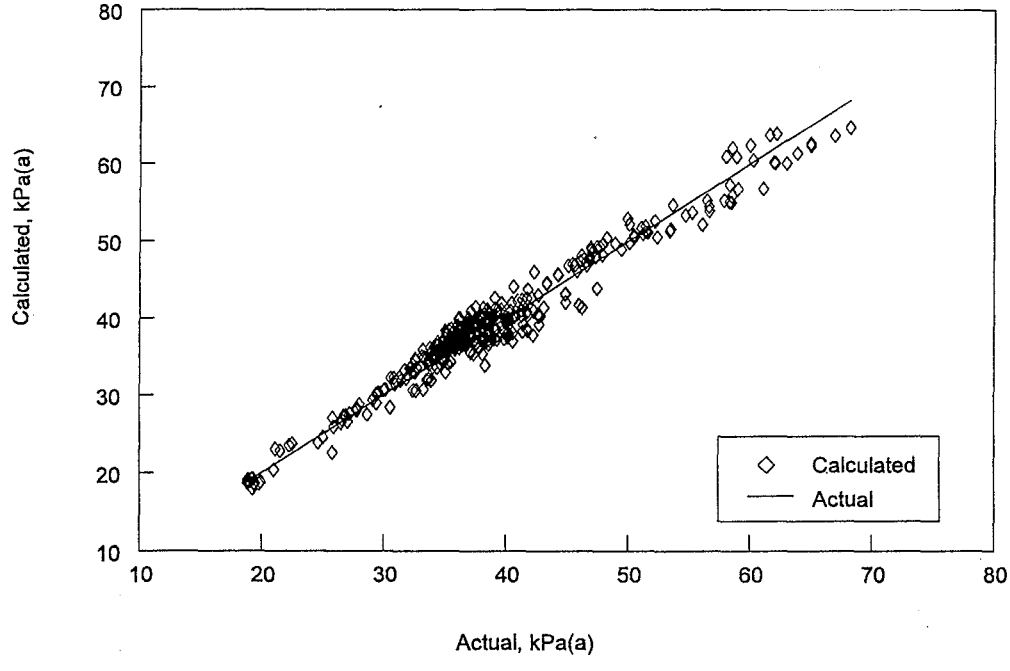


Figure 6.20 : Actual vs calculated n-butene partial pressure in the product gas - Case 5

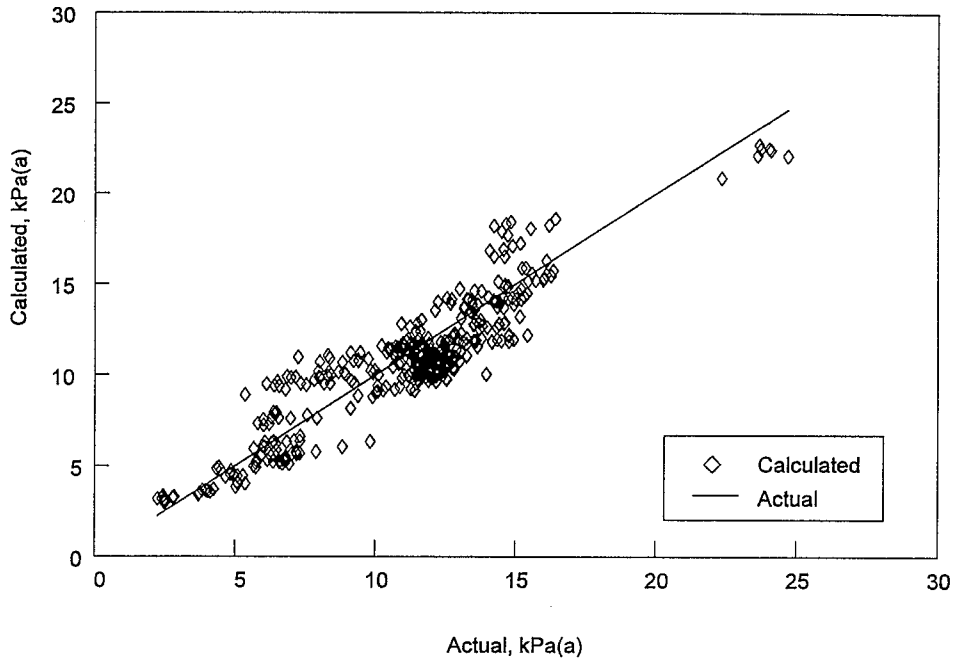


Figure 6.21 : Actual vs calculated isobutene partial pressure in the product gas - Case 5

### 6.2.6 CASE 6 : ADSORPTION OF N-BUTENE AND DESORPTION OF ISOBUTENE

For Case 6, it is assumed that the overall skeletal isomerisation rate is controlled by the net rate of the adsorption of the n-butene and the desorption of the isobutene. The surface reactions of n-butene / isobutene are assumed to be at equilibrium. The overall rate equation for Case 6 is

$$r = \frac{(S)_t \cdot \left( P_{n\text{-}c_4^=} - \frac{P_{i\text{-}c_4^=}}{K} \right)}{\left( \frac{1}{k_1} + \frac{1}{k_6 \cdot K} \right) + \left( \frac{1}{k_6 \cdot K} + \frac{1}{k_3 K_a} \right) \cdot K_a \cdot P_{n\text{-}c_4^=} + \left( \frac{1}{k_1 \cdot K_s} + \frac{1}{k_1} \right) \cdot \frac{P_{i\text{-}c_4^=}}{K_d}} \qquad 6\text{-}9$$

The optimum values of the unknown parameters and statistical parameters evaluated are shown in Table 6.6. The confidence contours and parity plots are shown in Figures 6.22 and 6.23 and Figures 6.24 to 6.25 respectively.

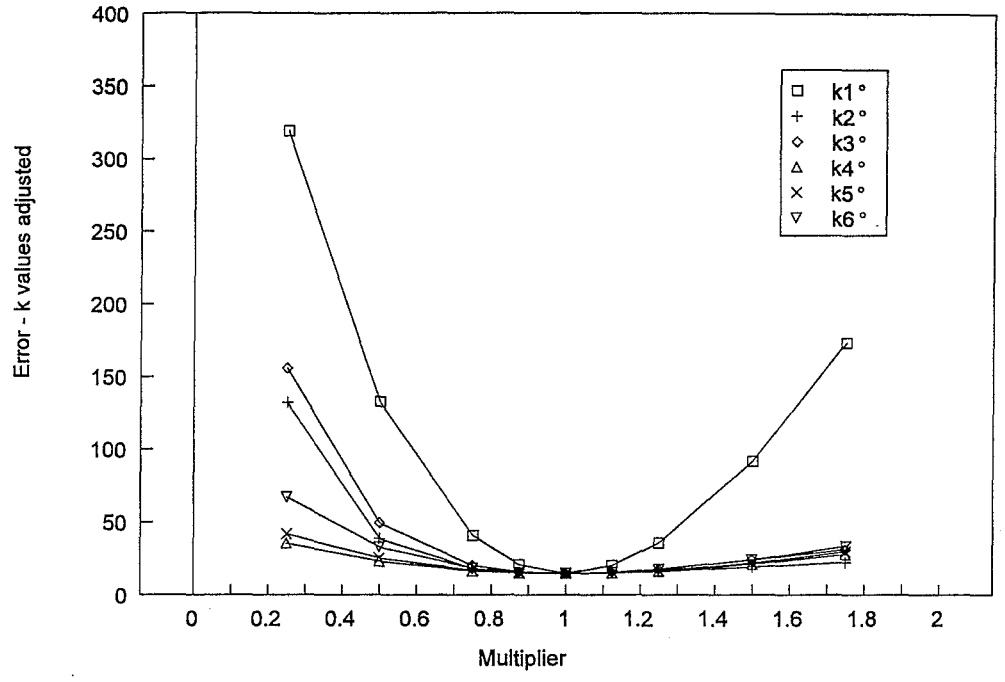


Figure 6.22 : Effect of adjusting individual $k_i°$ values on the overall percentage error when predicting the n-butene and isobutene partial pressures in the product gas for Case 6

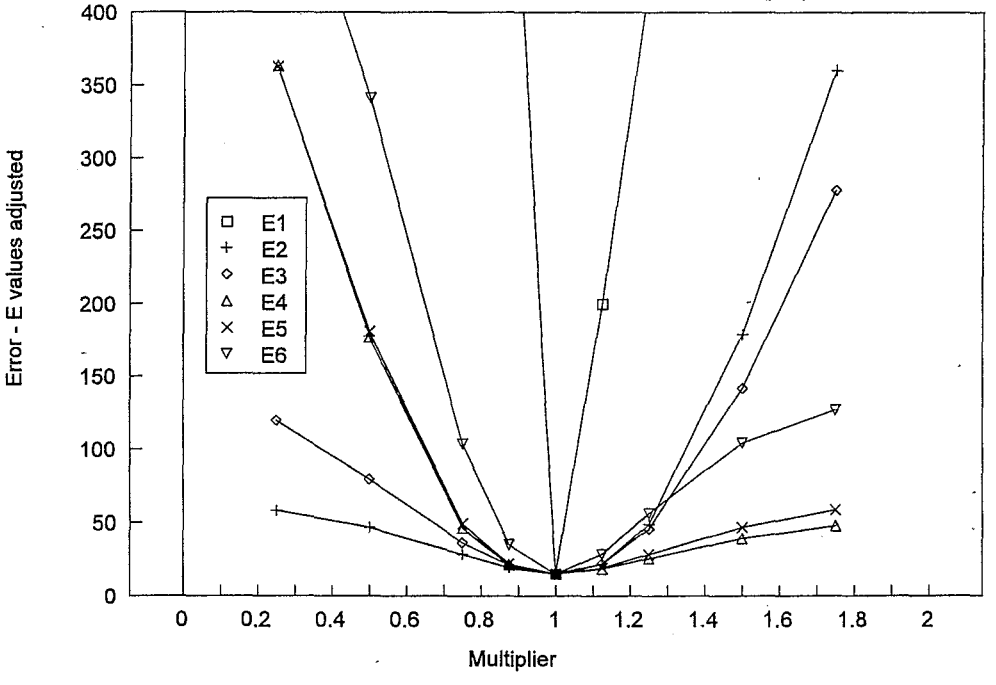


Figure 6.23 : Effect of adjusting individual E values on the overall percentage error in predicting the n-butene and isobutene partial pressures in the product gas - Case 6

Again, the shape of the contours confirms that for each parameter an optimum value was found. However, a global inspection of Figure 6.22 and Figure 6.23 suggests that the forward reaction rates must be larger than and the reverse reaction rates smaller than, some limiting value. The very symmetrical contour obtained for the parameters describing the rate of adsorption of n-butene, Step 1 in Figure 6.1, suggests this is a significant step.

The values of the unknown parameters, as determined using the procedure outlined in Appendix 5 and Chapter 5 are shown together with the results from the statistical investigations in Table 6.6. The ability of Case 6 to predict the performance of the bench reactor system was also confirmed visually by means of the parity plots shown in Figures 6.24 and 6.25.

**TABLE 6.6 : OPTIMUM VALUES OF THE KINETIC PARAMETERS : CASE 6**

**Units :** Pre Exponential Factor, $k_j^\circ$ = mol·kg$^{-1}$·s$^{-1}$·kPa$^{-1}$, Activation Energy $E_j$ = cal·mol$^{-1}$

| Pre - exponential factors | | Activation Energy | |
|---|---|---|---|
| $k_1^\circ$ | 0.118 (+1.19e-3 / -1.07e-3) | $E_1$ | 11921 (+3.57 / -1.24) |
| $k_2^\circ$ | 5.533 (+6.84e-1 / -4.73e-1) | $E_2$ | 5144 (+40.0 / -64.7) |
| $k_3^\circ$ | 1.423 (+9.37e-2 / -6.89e-2) | $E_3$ | 4172 (+31.5 / -37.9) |
| $k_4^\circ$ | 0.393 (+5.23e-2 / -4.66e-2) | $E_4$ | 5207 (+80.0 / -45.8) |
| $k_5^\circ$ | 1.471 (+1.64e-1 / -1.43e-1) | $E_5$ | 5170 (+64.5 / -39.8) |
| $k_6^\circ$ | 0.262 (+2.05e-2 / -1.68e-2) | $E_6$ | 7435 (+30.0 / - 20.1) |

| Parameter | $p_{n\text{-Butene}}$ | $p_{Isobutene}$ |
|---|---|---|
| Coefficient of Determination | 0.961 | 0.842 |
| Sum of Errors Squared | 0.772 | 9.257 |
| Lack of Fit | 0.341 < 1.0 Satisfactory fit | 0.795 < 1.0 Satisfactory fit |

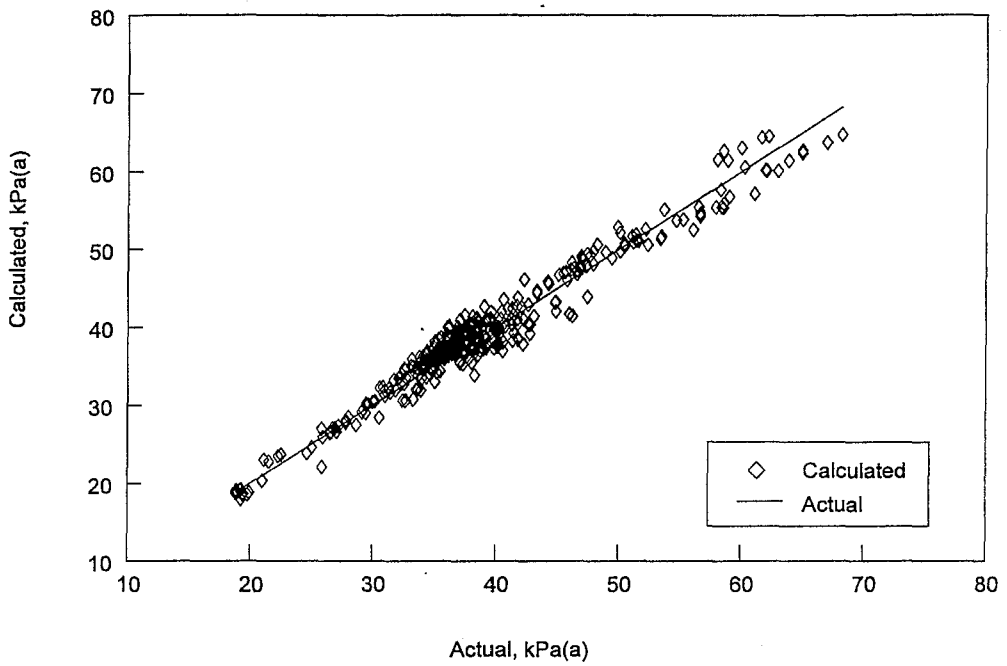


Figure 6.24 : Actual vs calculated n-butene partial pressure in the product gas - Case 6

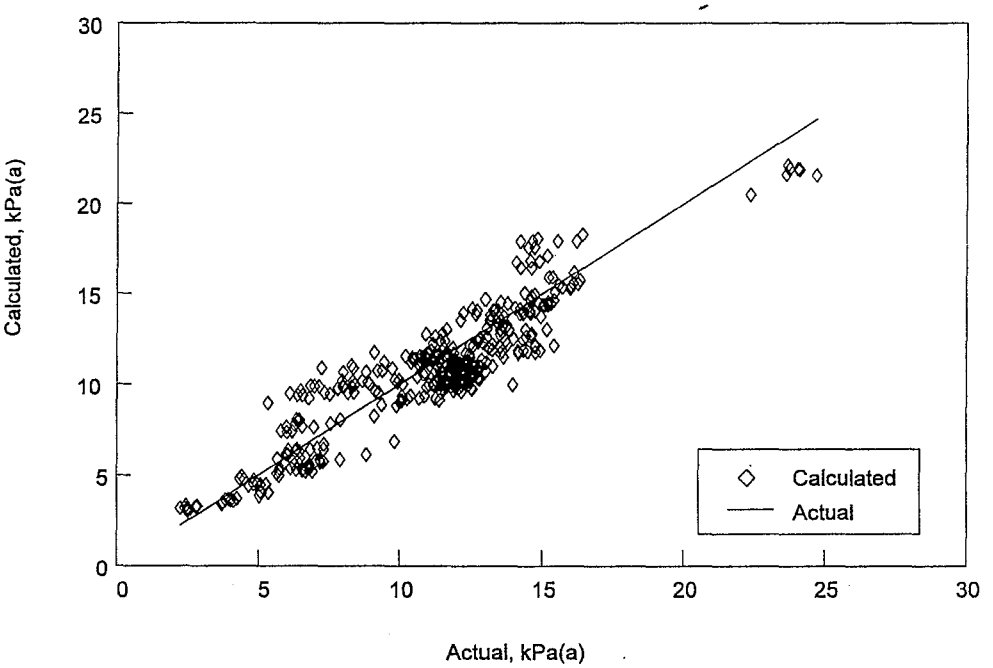


Figure 6.25 : Actual vs calculated isobutene partial pressure in the product gas - Case 6

### 6.2.7 CASE 7 : ADSORPTION OF N-BUTENE PLUS SURFACE REACTION OF N-BUTENE TO ISOBUTENE

For Case 7, it is assumed that the overall skeletal isomerisation rate is controlled by the net rate of the adsorption / desorption steps of the n-butene and the surface reaction rate of n-butene to isobutene. The desorption / adsorption reactions of the isobutene are assumed to be at equilibrium. The overall rate equation for Case 7 was developed to give

$$r = \frac{(S)_t \cdot \left( P_{n\text{-}c_4^=} - \frac{P_{i\text{-}c_4^=}}{K} \right)}{\left( \frac{1}{k_1} + \frac{1}{k_2 \cdot K_a} \right) + \left( \frac{1}{k_2 \cdot K_a} \right) \cdot K_a \cdot P_{n\text{-}c_4^=} + \left( \frac{1}{k_2 \cdot K_a} + \frac{K_s + 1}{k_1 \cdot K_s} \right) \cdot \frac{P_{i\text{-}c_4^=}}{K_d}} \qquad 6\text{-}10$$

The optimum values of the unknown parameters and statistical parameters evaluated are shown in Table 6.7. The confidence contours and parity plots are shown in Figures 6.26 and 6.27 and Figures 6.28 and 6.29 respectively.

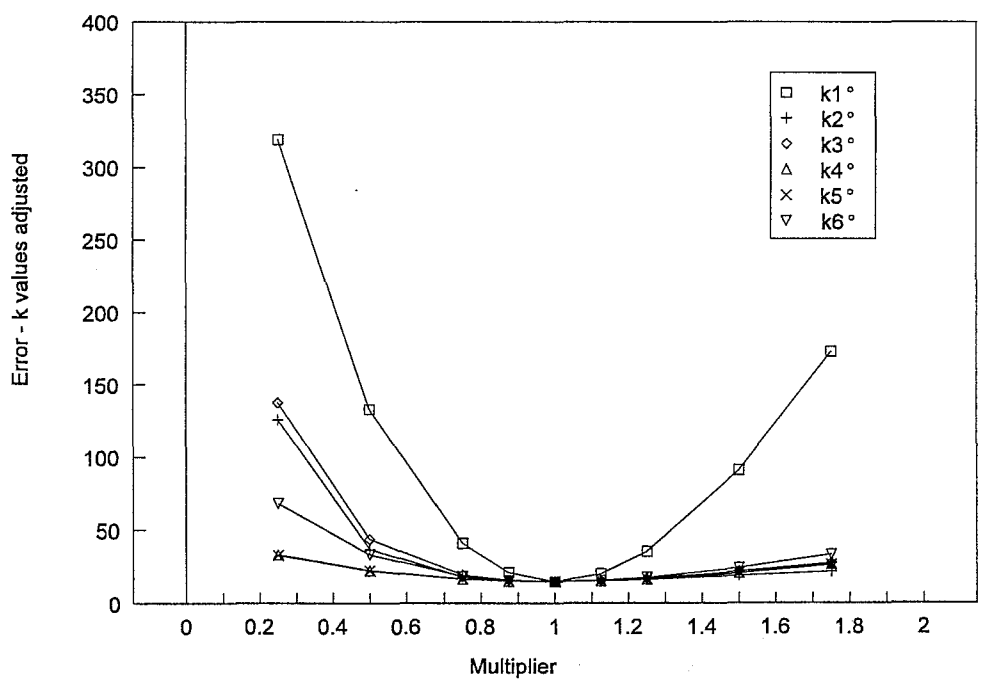


Figure 6.26 : Effect of adjusting individual $k_i°$ values on the overall percentage error when predicting the n-butene and isobutene partial pressures in the product gas for Case 7

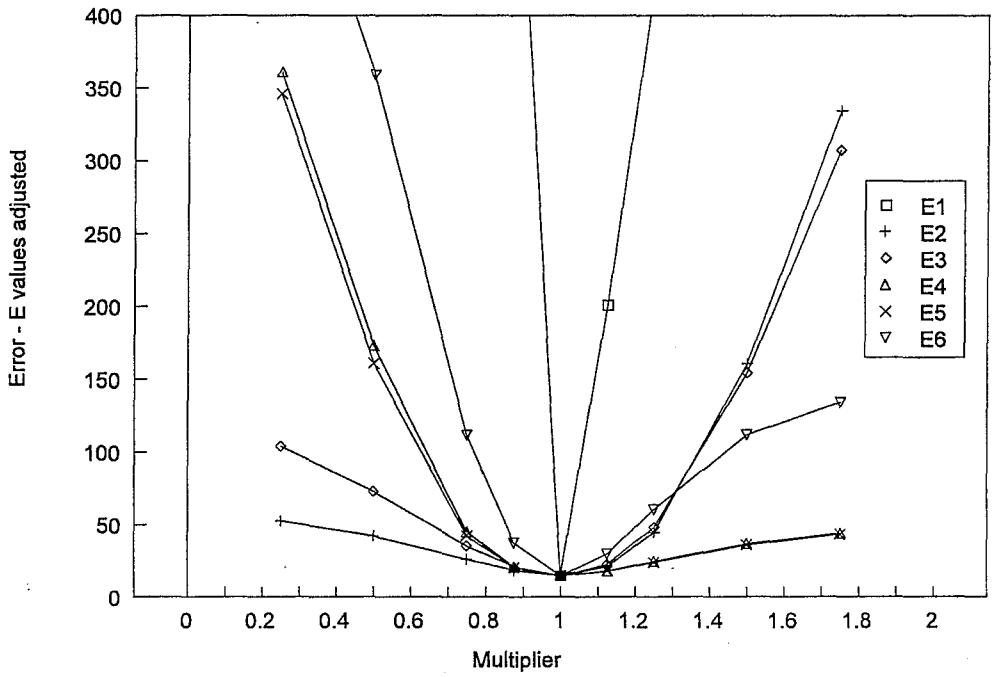


Figure 6.27 : Effect of adjusting individual E values on the overall percentage error in predicting the n-butene and isobutene partial pressures in the product gas - Case 7

From the contour plots, it may be seen that an optimum solution was located for each parameter. However, as was concluded previously, the very symmetrical nature of the confidence contours for the parameters required to describe the adsorption of n-butene, suggest that this is a significant reaction step. Furthermore, a global inspection of the confidence contours for the remaining reactions suggests that the rates of all forward reactions must be greater than, and the rates of the reverse reactions smaller than, some limiting value.

The values of the unknown parameters are shown together with the results from the statistical investigations in Table 6.6 from which it may be concluded that Case 7 is able to predict the performance of the bench reactor system. The ability of Case 7 to predict the performance of the bench reactor system was also confirmed visually by means of the parity plots shown in Figures 6.28 and 6.29.

**TABLE 6.7 : OPTIMUM VALUES OF THE KINETIC PARAMETERS : CASE 7**

**Units :** Pre Exponential Factor, $k_j^\circ$ = mol·kg$^{-1}$·s$^{-1}$·kPa$^{-1}$, Activation Energy $E_j$ = cal·mol$^{-1}$

| Pre - exponential factors | | Activation Energy | |
|---|---|---|---|
| $k_1^\circ$ | 0.120 (+1.24e-3 / -1.06e-3) | $E_1$ | 11962 (+3.56 / -1.23) |
| $k_2^\circ$ | 8.153 (+1.21 / -7.17e-1) | $E_2$ | 4989 (+44.4 / -75.3) |
| $k_3^\circ$ | 1.438 (+1.26e-1 / -8.25e-2) | $E_3$ | 4703 (+33.4 / -44.0) |
| $k_4^\circ$ | 0.400 (+5.44e-2 / -5.69e-2) | $E_4$ | 5286 (+90.3 / -48.4) |
| $k_5^\circ$ | 1.964 (+2.79e-1 / -2.90e-1) | $E_5$ | 5188 (+94.8 / -51.9) |
| $k_6^\circ$ | 0.291 (+2.16e-2 / -1.98e-2) | $E_6$ | 7842 (+28.9 / - 19.1) |

| Parameter | $p_{n\text{-Butene}}$ | $p_{Isobutene}$ |
|---|---|---|
| Coefficient of Determination | 0.961 | 0.842 |
| Sum of Errors Squared | 0.777 | 9.216 |
| Lack of Fit | 0.343 < 1.0 Satisfactory fit | 0.798 < 1.0 Satisfactory fit |

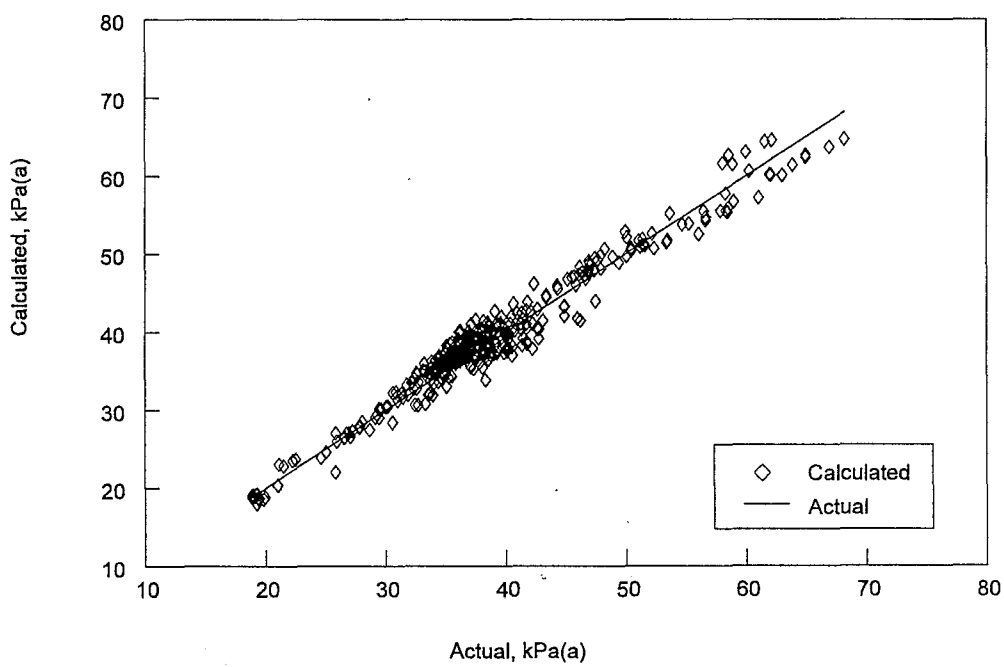


Figure 6.28 : Actual vs calculated n-butene partial pressure in the product gas - Case 7

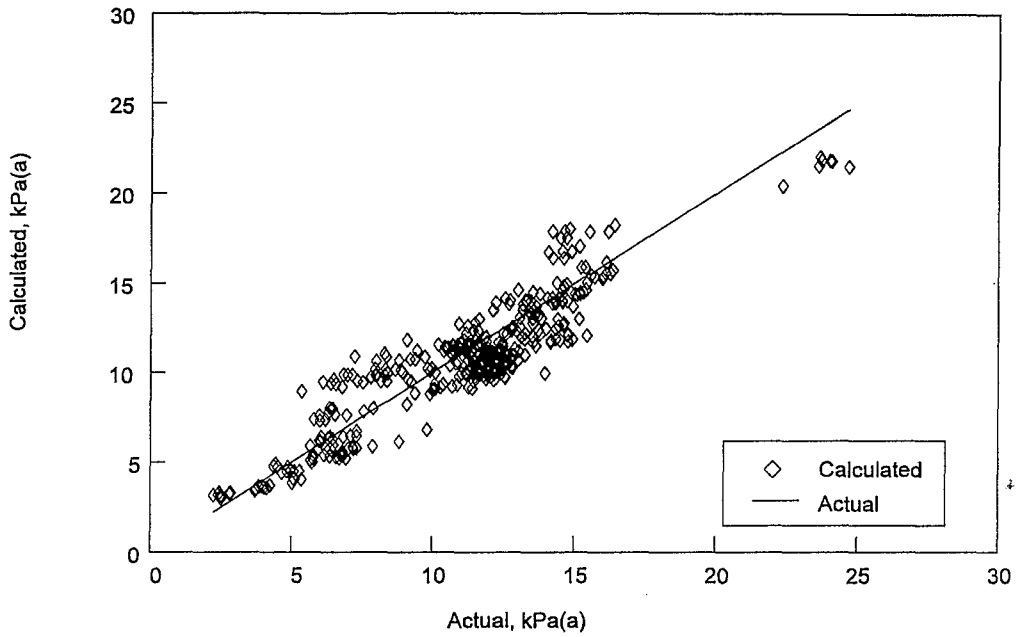


Figure 6.29 : Actual vs calculated isobutene partial pressure in the product gas - Case 7

### 6.2.8 CASE 8 : ADSORPTION OF N-BUTENE PLUS SURFACE REACTION OF N-BUTENE TO ISOBUTENE PLUS DESORPTION OF ISOBUTENE

For Case 8, it is assumed that the overall skeletal isomerisation rate (r) is equal to the net rate of the adsorption of the n-butene, the surface reaction rate of n-butene to isobutene and the desorption of the isobutene formed. Using the procedure presented in Appendix 3 the overall rate equation was developed to give

$$r = \frac{(S)_t \cdot \left( P_{n\text{-}C_4^=} - \frac{P_{i\text{-}C_4^=}}{K} \right)}{\left( \frac{1}{k_1} + \frac{1}{k_6 \cdot K} + \frac{1}{k_2 \cdot K_a} \right) + \left( \frac{1 + K_s}{k_6 \cdot K} + \frac{1}{k_2 \cdot K_a} \right) \cdot K_a \cdot P_{n\text{-}C_4^=} + \left( \frac{1}{k_2 \cdot K_a} + \frac{K_s + 1}{k_1 \cdot K_s} \right) \cdot \frac{P_{i\text{-}C_4^=}}{K_d}} \quad 6\text{-}10$$

The optimum values of the unknown parameters and statistical parameters evaluated are shown in Table 6.8. The confidence contours and parity plots are shown in Figures 6.30 and 6.31 and Figures 6.32 and 6.33 respectively.

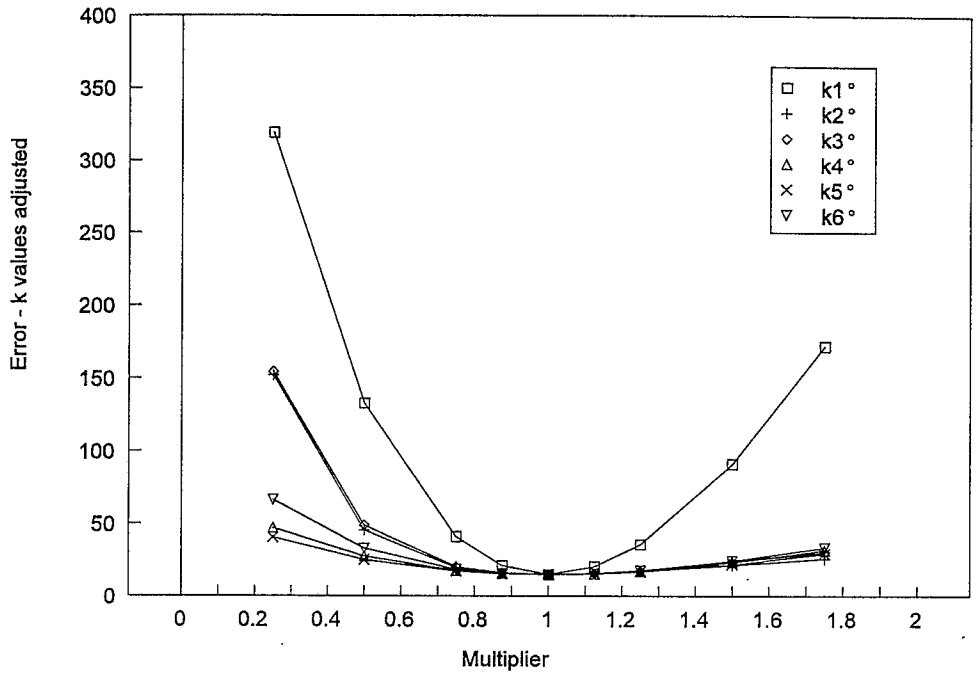


Figure 6.30 : Effect of adjusting individual $k_i°$ values on the overall percentage error when predicting the n-butene and isobutene partial pressures in the product gas for Case 8

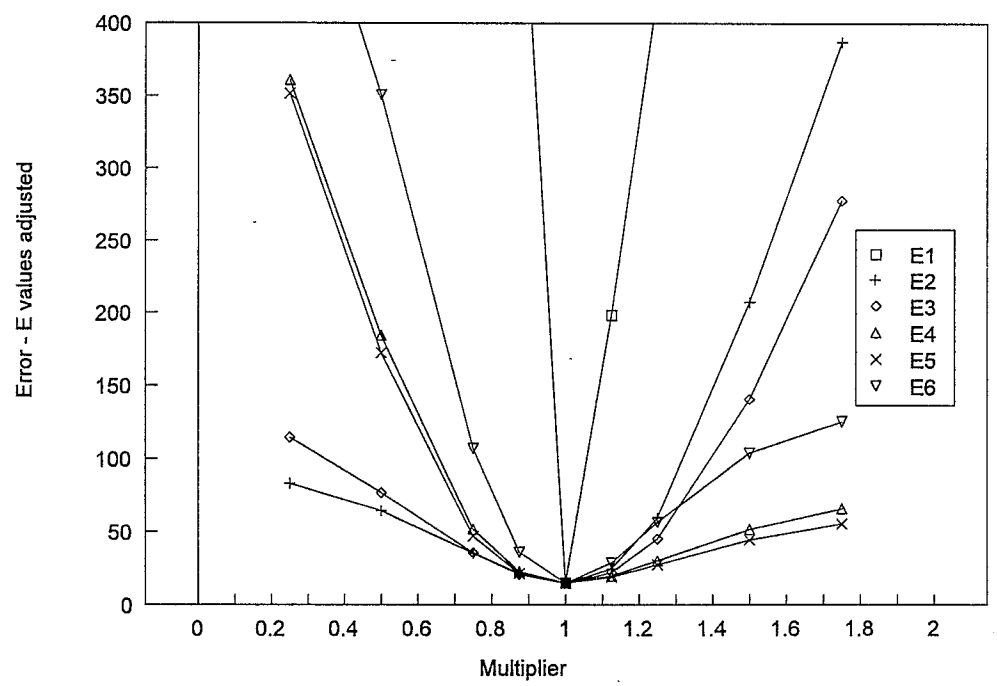


Figure 6.31 : Effect of adjusting individual E values on the overall percentage error in predicting the n-butene and isobutene partial pressures in the product gas - Case 8

Again, as was concluded previously, a global inspection of the confidence contours suggests that the adsorption of the n-butene is the significant step while the rates of all forward reactions must be greater than, and the rates of the reverse reactions smaller than, some limiting value.

The values of the unknown parameters are shown in Table 6.8 together with the results from the statistical analysis from which it may be concluded that Case 8 is capable of predicting the performance of the system. To further confirm the ability of Case 8 to predict the performance of the bench reactor system, parity plots of the actual and calculated n-butene and isobutene partial pressures in the product gas were prepared, as shown in Figures 6.32 and 6.33.

As may be seen from these figures Case 8 is indeed capable in predicting the performance of the bench reactor system with respect to the n-butene and isobutene partial pressures in the product gas.

**TABLE 6.8 : OPTIMUM VALUES OF THE KINETIC PARAMETERS : CASE 8**

**Units :** Pre Exponential Factor, $k_j^\circ$ = mol·kg$^{-1}$·s$^{-1}$·kPa$^{-1}$, Activation Energy $E_j$ = cal·mol$^{-1}$

| Pre - exponential factors | | Activation Energy | |
|---|---|---|---|
| $k_1^\circ$ | 0.123 (+1.25e-3 / -1.10e-3) | $E_1$ | 11850 (+3.58 / -1.26) |
| $k_2^\circ$ | 6.043 (+5.39e-1 / -3.68e-1) | $E_2$ | 5229 (+29.3 / -44.4) |
| $k_3^\circ$ | 1.608 (+1.10e-1 / -7.93e-2) | $E_3$ | 4175 (+32.1 / -39.4) |
| $k_4^\circ$ | 0.443 (+4.14e-2 / -3.71e-2) | $E_4$ | 5017 (+55.9 / -35.3) |
| $k_5^\circ$ | 1.212 (+1.37e-1 / -1.24e-1) | $E_5$ | 5053 (+68.4 / -41.7) |
| $k_6^\circ$ | 0.320 (+2.48e-2 / -2.09e-2) | $E_6$ | 7554 (+30.0 / - 19.7) |

| Parameter | $p_{n\text{-Butene}}$ | $p_{Isobutene}$ |
|---|---|---|
| Coefficient of Determination | 0.961 | 0.842 |
| Sum of Errors Squared | 0.773 | 9.262 |
| Lack of Fit | 0.341 < 1.0 Satisfactory fit | 0.796 < 1.0 Satisfactory fit |

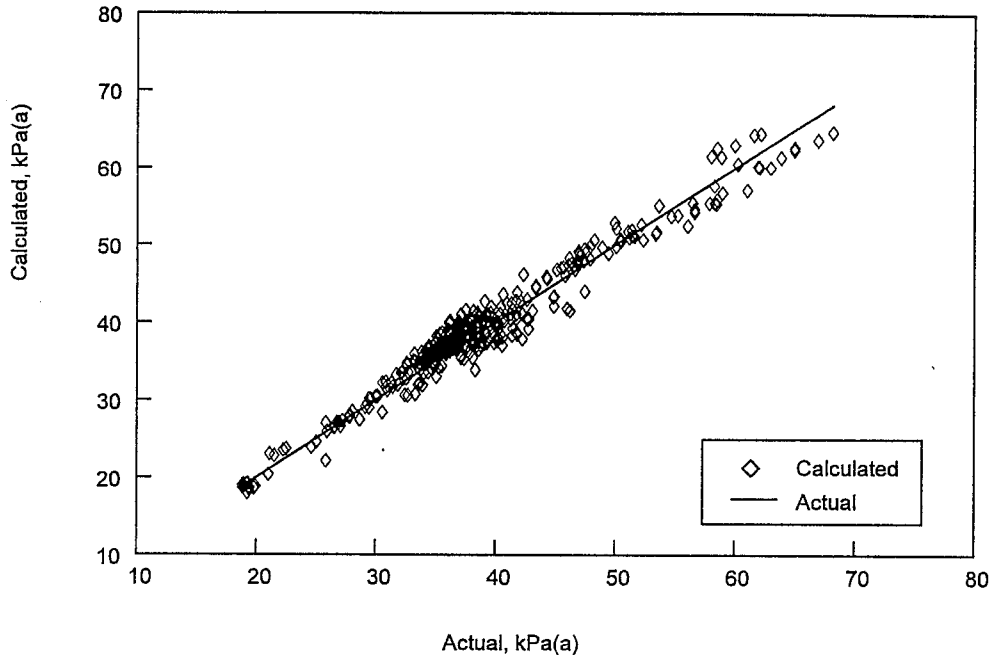


Figure 6.32 : Actual vs calculated n-butene partial pressure in the product gas - Case 8

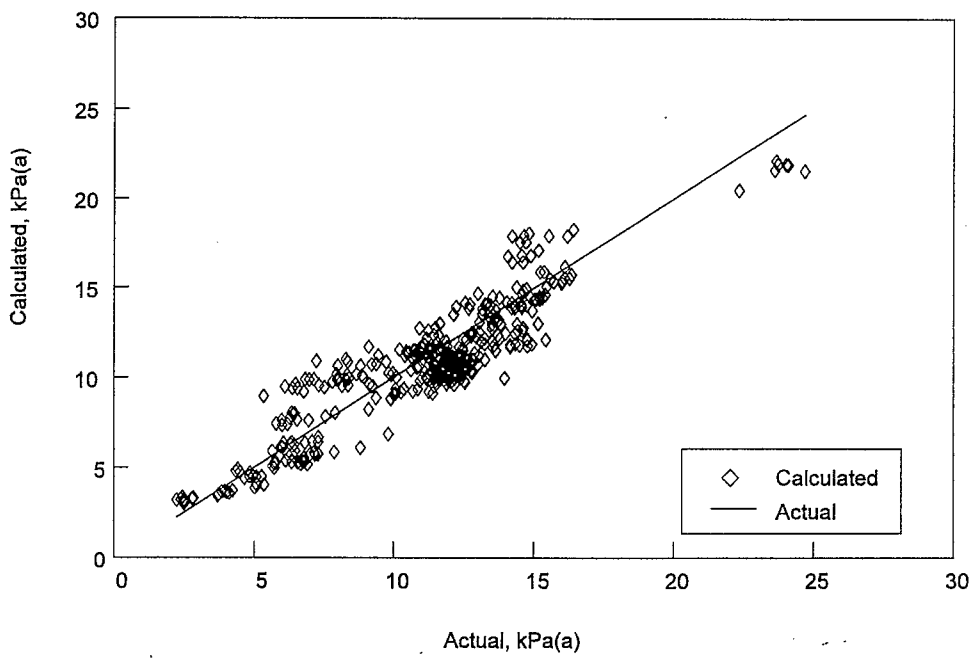


Figure 6.33 : Actual vs calculated isobutene partial pressure in the product gas - Case 8

### 6.2.9 SUMMARY

Using the procedures developed, as discussed in Chapter 5, Section 5.8 and Appendix 5, and a number of statistical tests, as discussed in Chapter 5, Section 5.9, the optimum values of the unknown parameters required by each of the rival models considered were determined and the accuracy of the calculated responses quantified. The results from the statistical analysis are summarised in Table 6.9, and the optimum values determined in each case, together with the confidence intervals, in Table 6.10.

**TABLE 6.9 : SUMMARY OF STATISTICAL RESULTS**

| Case | Coefficient of Determination | | Sum of errors squared | | Lack of Fit <1 Satisfactory | |
|---|---|---|---|---|---|---|
| | $p_{n\text{-Butene}}$ | $p_{Isobutene}$ | $p_{n\text{-Butene}}$ | $p_{Isobutene}$ | $p_{n\text{-Butene}}$ | $p_{Isobutene}$ |
| 1 | 0.960 | 0.832 | 0.761 | 9.658 | 0.339 | 0.830 |
| 2 | 0.961 | 0.842 | 0.776 | 9.215 | 0.343 | 0.796 |
| 3 | 0.961 | 0.842 | 0.771 | 9.244 | 0.341 | 0.795 |
| 4 | 0.961 | 0.842 | 0.769 | 9.406 | 0.339 | 0.798 |
| 5 | 0.961 | 0.842 | 0.769 | 9.343 | 0.340 | 0.800 |
| 6 | 0.961 | 0.842 | 0.772 | 9.257 | 0.341 | 0.795 |
| 7 | 0.961 | 0.842 | 0.777 | 9.216 | 0.343 | 0.798 |
| 8 | 0.961 | 0.842 | 0.773 | 9.262 | 0.341 | 0.796 |

Although some differences for different models were observed in the Coefficient of determination, the Sum of Errors Squared and the Lack of Fit, these were considered not to be significant enough to allow discrimination between rival models.

The same conclusion was reached, i.e., that it was not possible to discriminate between rival mechanisms using the statistical methods considered, when the models were fitted to the pilot plant data, data at the extremes of the experimental region, using data with only a 50 % approach to equilibrium or using average time on line data from the bench reactor or the pilot plant reactor systems.

**TABLE 6.10 : PRE EXPONENTIAL FACTORS AND ACTIVATION ENERGIES**

**Units :** Pre Exponential Factor, $k_j$° = mol·kg$^{-1}$·s$^{-1}$·kPa$^{-1}$, Activation Energy $E_j$ = cal·mol$^{-1}$

| | **Case 1** | | **Case 2** | |
|---|---|---|---|---|
| **Step,i** | $k_i'$° + / - Interval | $E'_i$ + / - Interval | $k_i$° + / - Interval | $E_i$ + / - Interval |
| 1 | **0.09** +7.9e-4 / -7.2e-4 | **11785** +3.3 / -0.96 | **0.12** + 1.2e-3 / -1.1e-3 | **12015** +3.6 / -1.2 |
| 2 | **0.63** +2.7e-2 / -2.5e-2 | **12979** +25.7 / -94.5 | **5.37** +9.4e-1 / -6.1e-1 | **5281** +51.0 / -89.6 |
| 3 | - | - | **1.06** +8.8e-2 / -6.2e-2 | **4569** +34.6 / -43.7 |
| 4 | - | - | **0.33** +6.2e-2 / -5.9e-2 | **5537** +11.6 / -58.7 |
| 5 | - | - | **1.51** +2.2e-1 / -2.1e-1 | **5260** +89.9 / -51.3 |
| 6 | - | - | **0.25** +1.9e-2 / -1.6e-2 | **7931** +27.8 / -18.9 |
| | **Case 3** | | **Case 4** | |
| **Step,i** | $k_i$° + / - Interval | $E_i$ + / - Interval | $k_i$° + / - Interval | $E_i$ + / - Interval |
| 1 | **0.11** +1.1e-3 / -1.0e-3 | **10975** +3.7 / -1.4 | **0.03** +7.5e-3 / -6.7e-4 | **12396** +3.5 / -1.2 |
| 2 | **2.68** +2.6e-2 / -2.3e-2 | **5826** +5.2 / -3.0 | **3.79** +3.4e-2 / -3.1e-2 | **5518** +5.2 / -3.0 |
| 3 | **1.53** +1.3e-1 / -9.2e-2 | **3522** +46.3 / -56.1 | **0.68** +5.4e-3 / -5.0e-3 | **4980** +5.1 / -2.9 |
| 4 | **1.45** +1.7e-2 / -1.1e-2 | **3939** +5.1 / -7.3 | **0.46** +5.2e-3 / -3.5e-3 | **5079** +3.8 / -5.9 |
| 5 | **0.31** +4.7e-2 / -4.3e-2 | **7286** +76.6 / -33.8 | **1.85** +1.9e-2 / -1.3e-2 | **4875** +3.5 / -5.7 |
| 6 | **0.73** +5.7e-2 / -4.7e-2 | **8017** +28.6 / -18.6 | **0.07** +5.4e-3 / -4.6e-3 | **10130** +27.2 / -12.6 |
| | **Case 5** | | **Case 6** | |
| **Step,i** | $k_i$° + / - Interval | $E_i$ + / - Interval | $k_i$° + / - Interval | $E_i$ + / - Interval |
| 1 | **0.07** +6.4e-4 / -5.7e-4 | **12034** +3.5 / -1.2 | **0.12** +1.2e-3 / -1.1e-3 | **1121** +3.6 / -1.2 |
| 2 | **3.19** +2.8e-2 / -2.6e-2 | **6148** +4.8 / -2.6 | **5.53** +6.8e-1 / -4.7e-1 | **5144** +40.0 / -64.7 |
| 3 | **0.93** +3.3e-2 / -2.5e-2 | **4416** +17.0 / -18.8 | **1.42** +9.4e-2 / -6.9e-2 | **4172** +31.5 / -37.9 |
| 4 | **0.51** +5.7e-3 / -3.8e-3 | **4663** +4.0 / -6.1 | **0.39** +5.2e-2 / -4.7e-2 | **5207** +80.0 / -45.8 |
| 5 | **0.92** +3.9e-2 / -3.2e-2 | **6303** +18.2 / -13.9 | **1.47** +1.6e-1 / -1.4e-1 | **5170** +64.5 / -39.8 |
| 6 | **0.18** +1.3e-2 / -1.1e-2 | **9397** +27.3 / -13.9 | **0.26** +2.1e-2 / -1.7e-2 | **7435** +30.0 / -20.1 |
| | **Case 7** | | **Case 8** | |
| **Step,i** | $k_i$° + / - Interval | $E_i$ + / - Interval | $k_i$° + / - Interval | $E_i$ + / - Interval |
| 1 | **0.12** +1.2e-3 / -1.1e-3 | **11962** +3.6 / -1.2 | **0.12** +1.3e-3 / -1.1e-3 | **11850** +3.6 / -1.3 |
| 2 | **8.15** +1.2e-1 / -7.2e-1 | **4989** +44.4 / -75.3 | **6.04** +5.4e-1 / -3.7e-1 | **5229** +29.3 / -44.4 |
| 3 | **1.44** +1.3e-1 / -8.3e-2 | **4703** +33.4 / -44.0 | **1.61** +1.1e-1 / -7.9e-2 | **4175** +32.1 / -39.4 |
| 4 | **0.40** +5.4e-2 / -5.7e-2 | **5286** +90.3 / -48.4 | **0.44** +4.1e-2 / -3.7e-2 | **5017** +55.9 / -35.3 |
| 5 | **1.96** +2.8e-1 / -2.9e-1 | **5188** +96.8 / -51.9 | **1.21** +1.4e-1 / 1.2e-1 | **5035** +68.4 / -41.7 |
| 6 | **0.29** +2.2e-2 / -2.0e-2 | **7842** +28.9 / -19.1 | **0.32** +2.5e-2 / -2.1e-2 | **7554** +30.0 / -19.7 |

Examining the absolute values of the pre-exponential factors and the activation energies for, the three forward and three backward elementary reaction steps considered, it was found that for a given step, these were similar irrespective of the assumption made as to the nature of the rate controlling step(s). This, together with the fact that it was not possible, on a statistical or visual basis by means of parity plots, to discriminate between rival models, suggests that the rates of the six elementary reaction steps considered and hence, the net rates of the adsorption, surface reaction and desorption steps, are similar.

From an examination of the confidence profiles generated, it was seen that in each case the model was equally sensitive to an increases or decreases in the values of the parameters used to describe the rate of n-butene adsorption (Step 1 in Figure 6.1). A symmetrical confidence contour is indicative, that a specific value is required. For the other two forward reactions, although the optimum values of the unknown parameters were found in each case, an overall view of the confidence contours suggested that the rate of the n-butene to isobutene surface reaction and the desorption of isobutene had to be larger than some limiting value. Similarly, for the reverse reactions, the adsorption of isobutene the isobutene to n-butene surface reaction and the desorption of n-butene, it was concluded that the rates had to be smaller than, some limiting value. It may be expected that in all cases the limiting value is the rate of the significant step, i.e., the adsorption of n-butene. The enthalpy and entropy for the adsorption equilibrium constants in the Hougen-Watson type rate equations, were not evaluated during this study. This is an area where further work is required. See also Boudart and Loffler (1990:317) and Arthur et al. (1991:8521).

To prove that a particular mechanism is the correct one, it must be shown that the family of curves representing the favoured mechanism fit the experimental data better than the other families, so that these can be rejected. With the large number of parameters involved, 4 for Case 1 and 12 for Cases 2 to 8, that can be chosen arbitrarily for each rate controlling step, an extensive experimental program would be required with very precise and reproducible data. It is not good enough to select the mechanism that best fits the data as differences may be so small as to be explained in terms of experimental error or statistical insignificance. In most cases the magnitude of the experimental error masks the differences predicted by the various mechanisms and so any number of alternative

mechanisms may fit the data equally well. We can therefore only select the mechanism which best fits the data with no guarantee that it is the correct mechanism. It may however be argued that once the correct mechanism has been found, the performance of the catalyst at previously untried operating conditions can be predicted. However, this is still dangerous as other resistances may become important, in which case the original rate equation is no longer valid. The emphasis, while studying the kinetics of the process, was not to enable extrapolation to operating conditions outside the defined region but to identify the intrinsic rate equation to enable the rigorous design of a commercial skeletal isomerisation reactor. With this in mind, the approach used, by among others, Choudhary and Doraiswamy (1975:234) and Bianchi et al. (1994:556), in evaluating not only the feasibility of the Hougan Watson type rate equations but the simple law of mass action as well, seems the correct one. Hence, as it was not possible on a statistical basis to reject any of the rival models, the simplest form of the rate equation, i.e., Case 1 - the law of mass action was selected.

## 6.3 FORMATION OF BY-PRODUCTS

At the conditions employed, 1-butene not only undergoes reversible bond isomerisation, i.e., the formation of *cis*-2- and *trans*-2-butene and skeletal isomerisation, i.e., the formation of isobutene, but also oligomerisation, cracking and hydrogenation / dehydrogenation reactions. The extent of by-product formation can be limited by the choice of catalyst and operating conditions. During this bench scale reactor study, starting with pure 1-butene, some by-products were formed. The by-products partial pressure in the product gas was on average less than 1.3 % of the system pressure. In comparison, the average n-butene, isobutene and water partial pressures in the flue gas were 25.3 %, 7.2 % and 66.2 % of the system pressure, respectively. In the pilot plant substantially more by-products were present both in the feed, on average 5.3 % of the total system pressure and in the product gas. The average by-product partial pressure in the product gas being 6.3 % of the total system pressure, while the average n-butene, isobutene and water partial pressures were 21.3 %, 7.0 % and 65.4 % of the system pressure, respectively. However, in both cases the increase in the by-product partial pressure was approximately 1 % of the total system pressure.

The formation of by-products was modelled using the average of the product gas composition and operating parameters recorded during the various experiments conducted in both the bench (32 experiments) and pilot (25 experiments) reactor systems. The optimum values of the parameters required to model the formation of the by-products, were generated simultaneously together with those required to model the rate of n-butene skeletal isomerisation. The latter, as was done previously by various workers was described using the law of mass action (Case 1). The rate of formation of the by-products was in turn expressed using

$$r_{bp} = k'' \cdot \exp\left(\frac{-E''}{R \cdot T}\right) \cdot P^{m}_{n\text{-}C_4} \qquad 6\text{-}11$$

where

k" is the frequency factor for the by-product reaction, k" = 0.072 mol·kg$^{-1}$·s$^{-1}$·kPa$^{-m}$,

E" is the activation energy for the by-product formation reaction, E" = 13425 cal·mol$^{-1}$,

m is the reaction order for the by-product formation equation, m = 0.778,

T is the system temperature, K,

R is the universal gas constant, R = 1.987 cal·mol$^{-1}$·K$^{-1}$ and

$P^{m}_{n\text{-}C4}$ is the n-butene partial pressure, kPa(a).

To confirm that the optimum values of the various parameters required to calculate the rate of by-product formation had indeed been located, the effect of adjusting each of the values, on the overall percentage error, was determined, as shown in Figure 6.34. As may be seen from Figure 6.34, the percentage error remains approximately constant before increasing rapidly as the value of the power (m) was increase, while for the activation energy (E") the inverse behaviour was observed. These trends suggest that the value of the power (m) must be smaller than, and the activation energy (E") must be larger than some limiting value, both of which imply that the by-product formation rate must be smaller than some limiting value. This, combined with the fact that the regions where the error appears to be independent of changes in either m or E" overlap, suggest that a number of combinations of m and E" could be used to model the rate of by-product formation. Changes in the pre-exponential factor, k", had little effect on the overall error.

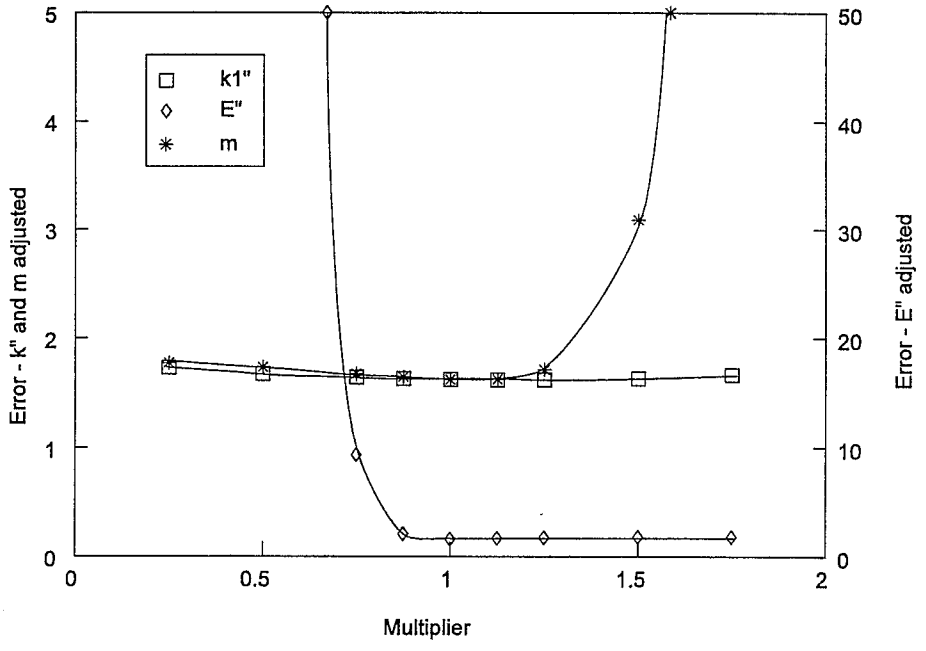


Figure 6.34 : Effect of adjusting the values of E", k" and m on the overall percentage error when predicting the by-product partial pressure in the product gas

The ability of the proposed model was confirmed by means of a parity plot of the actual and calculated by-product partial pressure in the product gases from the pilot plant and the bench reactor systems, as shown in Figure 6.35.

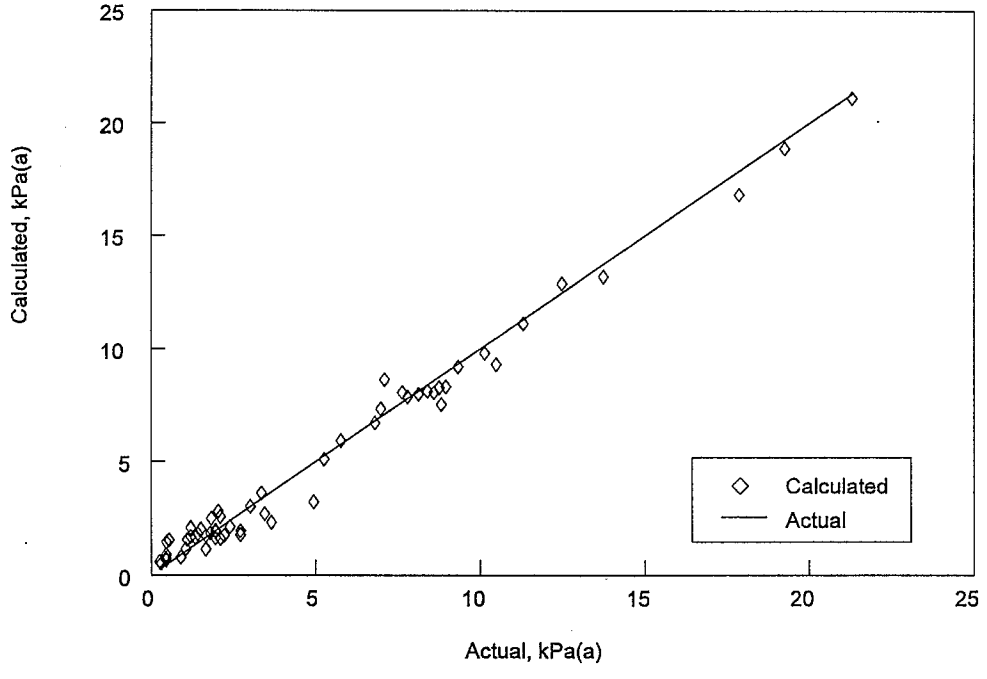


Figure 6.35 : Actual vs calculated pilot plant and bench reactor average time on line by-product partial pressure in the product gas

To reduce the number of unknowns, while determining the optimum values of the various parameters required for each of the n-butene skeletal isomerisation rate equations considered during this study, the parameters required to describe the formation of the by-products were fixed at the values reported previously.

## 6.4 PREDICTION OF THE PILOT PLANT PERFORMANCE

The emphasis, while studying the kinetics of the n-butene skeletal isomerisation reaction was to identify the intrinsic rate equation to enable the rigorous design of a commercial skeletal isomerisation reactor. With this in mind, and as it was not possible to distinguish between rival models on a statistical basis, the suitability of the simplest form of the rate equation, the law of mass action, in predicting the performance of the pilot plant was investigated. Using the program developed, together with the values of the unknown parameters determined previously, the average time on line performance of the pilot plant was calculated. The results obtained were compared to the actual values by means of parity plots as shown in Figure 6.36 to Figure 6.38.

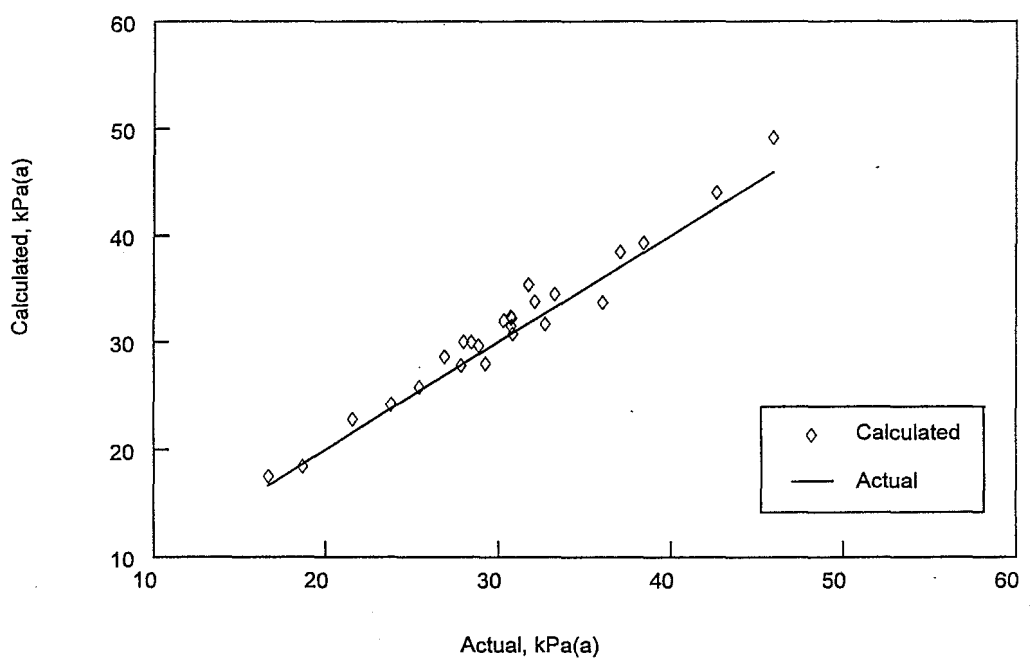


Figure 6.36 : Actual vs calculated n-butene partial pressure in the pilot plant product gas calculated using the kinetic model (Case 1) developed from the bench reactor data

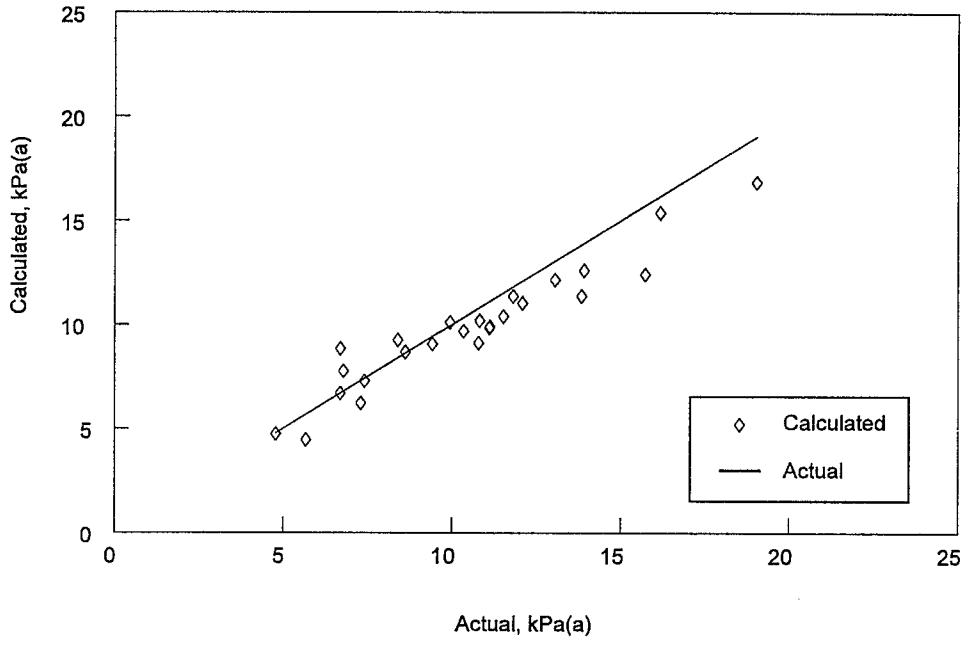


Figure 6.37 : Actual vs calculated isobutene partial pressure in the pilot plant product gas calculated using the kinetic model (Case 1) developed from the bench reactor data

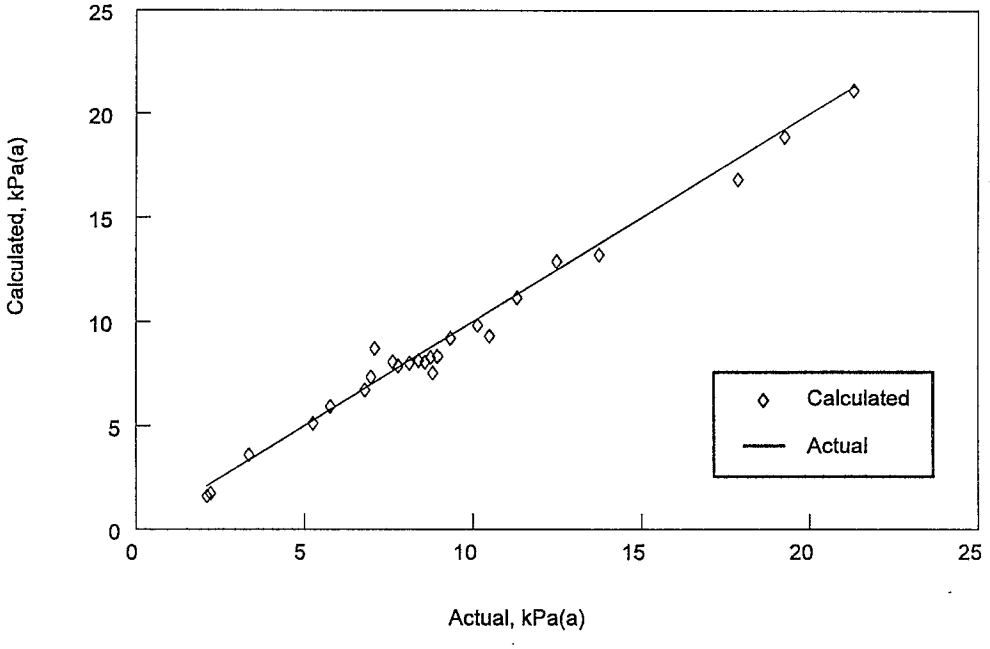


Figure 6.38 : Actual vs calculated by-products partial pressure in the pilot plant product gas calculated using the model developed from bench and pilot reactor data

A closer examination of Figures 6.36 and Figure 6.37 suggests that at the extremes, the model under predicts the performance of the pilot plant. At the upper limit of the n-butene partial pressure considered during this investigation of almost 45 kPa(a), the calculated n-butene partial pressure is approximately 5 kPa(a) above the actual value. Hence, at the upper extreme, the model prediction is conservative. However, at the envisaged commercial conditions the n-butene partial pressure in the product gas will on average be 30 kPa(a). As may be seen from Figure 6.36, the model accurately predicts the performance of the pilot plant near this point. It was therefore concluded that the model developed using the bench scale reactor system is suitable for predicting the performance of the pilot plant and the rigorous design of the commercial reactor.

## 6.5 CONCLUSIONS

Using the bench scale reactor system, the rate of the n-butene skeletal isomerisation to isobutene in the absence of other resistances, was measured. The various rate equations, based on the mono-molecular mechanism (Choudhary and Doraiswamy, 1975:235), when a single step, or multiple steps, control the overall reaction rate were, developed (See also Appendix 3). Next, using the FORTRAN program set up (See Appendix 5), the optimum values of the unknown parameters for each of the rate equations were determined. That in each case the optimum values of the unknown parameters were found was confirmed by an examination of the confidence contours set up. It was found that the seven mechanistic rate equations developed, and the law of mass action, were equally capable in predicting the performance of the bench scale reactor system. Discrimination on a statistical basis, using a number of procedures as discussed by (Sarup and Wojchiehowski, 1989:70, Draper and Smith, 1981:533, Box et al., 1978:43) was not possible.

However, it was found that for a given step the absolute values of the pre-exponential factors and the activation energies for the three forward and three backward elementary reaction steps considered, were similar, irrespective of the assumption made as to the nature of the rate controlling step(s). It was thus concluded that the rates of the six elementary reaction steps considered and hence, the net rates of the adsorption, surface reaction and desorption steps, are very similar. In view of this, the fact that it was not

possible to discriminate between models developed by assuming that a specific reaction step(s) controls the overall rate, may be understood. Using multi-step modelling to identify the n-butene skeletal isomerisation mechanism has not previously been reported in the literature.

From an examination of the confidence profiles generated, it was found that in each case the model were equally sensitive to increases or decreases in the values of the parameters used to describe the rate of n-butene adsorption (Step 1 in Figure 6.1). A symmetrical confidence contour is indicative, that a specific value is required. It may thus be proposed that the rate of n-butene adsorption on a single site on the surface of the catalyst is the most significant reaction step. This mechanism was previously proposed by Choudhary and Doraiswamy (1975:234) while studying a fluorinated alumina catalyst at temperatures below 435°C. At higher temperatures, they observed a switch in the mechanism, with isobutene desorption becoming the rate controlling step. For the other two forward reactions, although the optimum values of the unknown parameters were found in each case. However, taking a global view of the confidence contours, suggested that the rate of the n-butene to isobutene surface reaction, and the desorption of isobutene, have to be larger than some limiting value. Similarly, for the reverse reactions, the adsorption of isobutene, the isobutene to n-butene surface reaction and the desorption of n-butene, it was concluded that the rate had to be smaller than, some limiting value. It may be expected that the limiting value in all cases is the rate of the significant step, i.e., the adsorption of n-butene. The use of confidence contours to confirm that the optimum values of the unknown parameters had been found, or to assist in identifying the most significant reaction step, was not previously proposed in the literature.

During this investigation, the ratios of the n-butene, *cis*-2-, *trans*-2- and 1-butene in the flue gas were as predicted from thermodynamics. Hence, the linear butenes were treated as a single component, n-butene. This approach was previously used by, among others, Bianchi et al. (1994:554), Simon et al. (1994:480) and Choudhary and Doraiswamy (1971:55). This approach was not used by Szabo et al. (1993:323), who set up a set of elementary first order reactions to describe the bond as well as the skeletal isomerisation of the butenes. What has not previously been reported in the literature is an attempt to identify the overall reaction mechanism, using multi-step modelling of the butene bond and

skeletal isomerisation reactions as well as the formation of the by-products. The latter are traditionally assumed to form via the disproportionation of the butenes (Bianchi et al., 1994:556, Houžvička et al., 1996:288, Mériaudeau et al, 1997:L1), and are routinely treated as a single pseudo-component.

Hence, as discrimination between rival models was not possible, the simplest of the rate equations developed, based on the law of mass action, to describe the skeletal isomerisation of the n-butene to isobutene, as was previously reported by (Choudhary and Doraiswamy, 1971:55, Bianchi et al., 1994:554, Simon et al., 1994:480, Szabo et al., 1993:319) was adopted. The robustness of the rate equation developed and its suitability for the rigorous design of a commercial n-butene skeletal isomerisation reactor was further confirmed by the ability of this model to predict the performance of the pilot plant. The final form of the rate equation, together with the appropriate values of the unknown parameters, is repeated below.

The net rate of n-butene formation may be calculated using

$$r_{n\text{-}C_4^=} = -r_{ISOM} - r_{BP} \qquad 6\text{-}12$$

with the rate of the n-butene skeletal isomerisation using

$$r_{ISOM} = k'_1 \cdot \exp\left(\frac{-E'_1}{R \cdot T}\right) \cdot P_{n\text{-}C_4^=} - k'_2 \cdot \exp\left(\frac{-E'_2}{R \cdot T}\right) \cdot P_{i\text{-}C_4^=} \qquad 6\text{-}13$$

and the formation of by-products using

$$r_{BP} = k'' \cdot \exp\left(\frac{-E''}{R \cdot T}\right) \cdot P^{m}_{n\text{-}C_4^=} \qquad 6\text{-}14$$

where

$k''$ is the frequency factor for the by-product reaction, $k'' = 0.072$ mol·kg$^{-1}$·s$^{-1}$·kPa$^{-m}$,

$E''$ is the activation energy for the by-product formation reaction, $E'' = 13425$ cal·mol$^{-1}$,

$m$ is the order of the by-product formation equation, $m = 0.778$,

$k'_1$ is the frequency factor for the forward n-butene skeletal isomerisation reaction, $k'_1 = 0.095$ (+7.93e-4 / -7.22e-4) mol·kg$^{-1}$·s$^{-1}$·kPa$^{-1}$,

$k'_2$ is the frequency factor for the backward n-butene skeletal isomerisation reaction, $k'_2 = 0.631$ (+2.68e-2 / -2.48e-2) mol·kg$^{-1}$·s$^{-1}$·kPa$^{-1}$,

$E'_1$ is the activation energy for the forward n-butene skeletal isomerisation reaction, $E'_1 = 11785$ (+3.31 / - 0.96) cal·mol$^{-1}$,

$E'_2$ is the activation energy for the backward n-butene skeletal isomerisation reaction, $E'_2 = 12979$ (+25.7 / -94.5 )cal·mol$^{-1}$,

$T$ is the system temperature, K and

$R$ is the universal gas constant, $R = 1.987$ cal·mol$^{-1}$·K$^{-1}$.

Great care was taken during this study, as discussed in Chapter 5, to ensure that the kinetics of the system could be measured in the absence of other resistances. This, together with the fact that the values of the forward ($E_1 = 11785$ cal·mole$^{-1}$ = 49.3 kJ·mole$^{-1}$) and reverse ($E_2 = 12979$ cal·mole$^{-1}$ = 54.33 kJ·mole$^{-1}$) activation energy, are of a magnitude similar to those reported previously in the literature, from 35.2 kJ·mol$^{-1}$ to 113 kJ·mole$^{-1}$, (See also Section 2.3.8), confirms that they represent the true intrinsic activation energy for the n-butene skeletal isomerisation reaction over the silica alumina catalyst used during this study. The physical reasonableness of the enthalpy and entropy for the adsorption equilibrium constants in the Hougen-Watson type rate equations, were not evaluated during this study. This is an area where further work is required. See also Boudart and Loffler (1990:317) and Arthur et al. (1991:8521).